Chemical Science

ROYAL SOCIETY OF CHEMISTRY

PERSPECTIVE

View Article Online
View Journal | View Issue

Cite this: *Chem. Sci.*, 2020, **11**, 10571

All publication charges for this article have been paid for by the Royal Society of Chemistry

Received 25th June 2020
Accepted 19th August 2020

DOI: 10.1039/d0sc03528a

rsc.li/chemical-science

From CO_2 activation to catalytic reduction: a metal-free approach

Sreejyothi P. and Swadhin K. Mandal *

Over exploitation of natural resources and human activities are relentlessly fueling the emission of CO_2 in the atmosphere. Accordingly, continuous efforts are required to find solutions to address the issue of excessive CO_2 emission and its potential effects on climate change. It is imperative that the world looks towards a portfolio of carbon mitigation solutions, rather than a single strategy. In this regard, the use of CO_2 as a C1 source is an attractive strategy as CO_2 has the potential to be a great asset for the industrial sector and consumers across the globe. In particular, the reduction of CO_2 offers an alternative to fossil fuels for various organic industrial feedstocks and fuels. Consequently, efficient and scalable approaches for the reduction of CO_2 to products such as methane and methanol can generate value from its emissions. Accordingly, in recent years, metal-free catalysis has emerged as a sustainable approach because of the mild reaction conditions by which CO_2 can be reduced to various value-added products. The metal-free catalytic reduction of CO_2 offers the development of chemical processes with low cost, earth-abundant, non-toxic reagents, and low carbon-footprint. Thus, this perspective aims to present the developments in both the reduction and reductive functionalization chemistry of CO_2 during the last decade using various metal-free catalysts.

1. Introduction

The dream of a decarbonized economy is realistically far from reality since the global energy-related CO_2 emissions over the last 120 years have continuously increased with a few sporadic dips.[1a] For example, the global CO_2 emissions are expected to drop by 8% in 2020, which will be the lowest since 2010.[1b] This sharp decline in CO_2 emission comes at the expense of the COVID-19 pandemic, which has resulted in a severe health crisis and tremendous economic hardship globally, restricting human activities and hence is not sustainable.

Department of Chemical Sciences, Indian Institute of Science Education and Research-Kolkata, Mohanpur-741246, India. E-mail: swadhin.mandal@iiserkol.ac.in

Sreejyothi P. obtained her dual BS-MS degree majoring in Chemical Sciences from the Indian Institute of Science Education and Research (IISER) Kolkata in 2016. In the same year, she started her PhD under the supervision of Prof. Swadhin K. Mandal at IISER Kolkata. She has extensive expertise in handling low-valent main group compounds and her current research interest deals with CO_2 activation using low-valent phosphorus compounds.

Dr Swadhin K. Mandal is currently a Professor in the Department of Chemical Sciences at the Indian Institute of Science Education and Research Kolkata. He obtained his Doctoral Degree under supervision of Prof. S. S. Krishnamurthy from the Indian Institute of Science, Bangalore. He was a Postdoctoral Fellow in the Department of Chemistry at the University of California, Riverside, USA with Prof. Robert C. Haddon and an Alexander von Humboldt Fellow at the University of Göttingen, Germany with Prof. Herbert W. Roesky. His current research interests include organometallic catalysis using base metals and main-group metals with emphasis on developing transition metal-mimicking catalysts. He was awarded the prestigious Shanti Swarup Bhatnagar Prize in Chemical Sciences for 2018.

In 2019, the carbon dioxide emissions from anthropogenic activity reached 34 Gt,[1c] and Fig. 1 presents the steady increase in CO_2 emission over the last two decades. The CO_2 emissions from power plants and other industrial facilities are considered primarily as a waste product and liability. Accordingly, to address the issue of CO_2 emissions and their potential effects on climate change, society must continue to accelerate the exploitation of new energy technologies. It has been predicted that the CO_2 emissions need to decline by at least 50% to restrict an increase in the global average temperature by 2 °C by the year 2050.[2] Consequently, single technology solution is not expected to resolve this issue, rather the world will require a portfolio of carbon mitigation solutions relying on low-carbon or zero-carbon energy sources. Thus, one of the options that may be beneficial in achieving this target is the carbon capture and storage (CCS), which is being considered worldwide.[3a–c] CCS technologies have the potential to mitigate a significant amount of CO_2; however, the storage of captured carbon faces multiple challenges in terms of economic viability. Hence, recently, a relatively new alternative of carbon capture and recycling (CCR) has been gaining momentum. CCR involves the transformation of CO_2 into fuels and chemicals, while creating an added value, and thus can compensate the cost of its capture. In this regard, CO_2 is considered an attractive carbon feedstock in chemical synthesis since it is non-toxic, increasingly abundant, and environmentally well-distributed. Among the chemical processes, the reduction of CO_2 into various chemicals such as formic acid and methanol or light hydrocarbons such as methane is an extremely useful conversion owing to the wide applications of these products such as hydrogen carriers and their direct use as fuels. Thus, the reduction of CO_2 into various energy intensive chemicals and fuels is considered to have the most potential for chemical transformation of CO_2.[4,5] However, it should be noted that the current use of CO_2 in chemical synthesis is very limited,[4,6] which may be overcome by addressing two major issues. Firstly, the high kinetic and thermodynamic stability of CO_2 requires suitable catalysts for its reduction. Traditionally, over the years, various homogenous and heterogeneous methods have been developed for the catalytic reduction of CO_2 mainly using transition metal-based catalysts under harsh reaction conditions.[7–11] The transition metals used in the catalytic reduction of CO_2 are usually rare, and hence expensive, and also toxic to the environment. Secondly, the economics of the catalytic process must be competitive with the products obtained from the petrochemical industry. This may be achieved by replacing the expensive transition metals with metal-free catalysts operating under mild conditions. An ideal catalyst will ensure that the activation energy remains low, and thus the overall carbon balance is not compromised by the thermal loading since the energy input should be as carbon-free as possible. In recent years, metal-free catalysis along with transition metal-based catalysis have emerged as a sustainable approach because of the milder reaction conditions under which CO_2 can be reduced into various value-added products using boranes and silanes as reductants. The metal-free catalytic reduction of CO_2 can allow the development of chemical processes with low cost, earth-abundant, non-toxic reagents, and a significantly reduced carbon-footprint.

In this regard, it is worth mentioning that excellent reviews are available in literature, which either highlighted reduction or reductive functionalization of CO_2.[6,11–20] However, a detailed article covering the activation, reduction and reductive functionalization of CO_2 in an integrated way using metal-free catalysts and reducing agents such as boranes, silanes and hydrogen is lacking. Thus, this perspective aims at documenting these developments in both the reduction and reductive functionalization chemistry of CO_2 during the last decade using metal-free catalysts. We begin by highlighting the various activation modes of CO_2 by major classes of metal-free systems. The various conceptual aspects of CO_2 activation are described and correlated with how metal-free systems can mimic transition metals. This understanding is considered to be fundamental in the design of appropriate catalysts. Subsequently, two aspects of the reduction chemistry of CO_2 are widely covered. The first part deals with recent developments in the reduction of CO_2 into formic acid, methanol and methane. The second part documents the catalytic reduction of CO_2 together with its functionalization, forming new C–N bonds to yield *N*-formylamines, *N*-formylamides, *N*-methylamines and aminals.

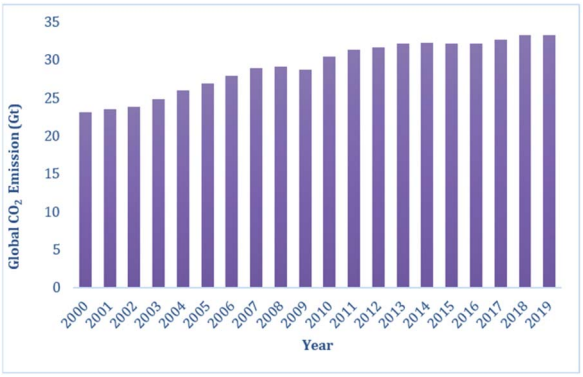

Fig. 1 Energy-related global CO_2 emission in the last two decades.[1c]

2. Activation of CO_2 by various metal-free systems

The activation of CO_2 molecules is an uphill task owing to its high thermodynamic and kinetic stability.[21] Nevertheless, this process is considered to be the key step in the design of any catalytic process for the conversion of CO_2 into value-added products. Although CO_2 has a zero dipole moment, it is a charge-separated molecule with an inherent difference in polarity between its oxygen and carbon atoms. Thus, in contrast to other inert molecules, such as N_2, the presence of this internal dipole along the C–O bonds makes the CO_2 molecule ambiphilic in nature. The HOMO of the CO_2 molecule is centred on the oxygen atoms, while its LUMO is located on the carbon atom. Consequently, the carbon centre is susceptible to nucleophilic attack, while the oxygen centres can interact with

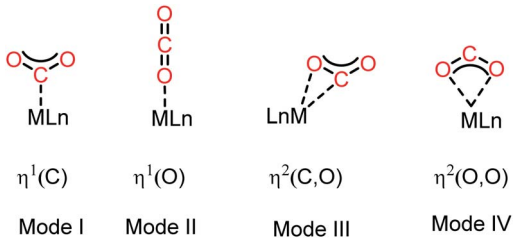

Fig. 2 Common binding modes of the CO_2 molecule with metal (considering a single metal).

electrophiles. Traditionally, transition metal-based catalysts have been considered as the most efficient for activation of CO_2 owing to their ability to interact with CO_2 molecules in various ways. In this regard, the most common strategy for CO_2 activation involves coordination with metal ions. The commonly observed binding modes of CO_2 with metals are demonstrated in Fig. 2.[22] One of the most common binding modes involves η^1–(C) bonding, in which the metal activates CO_2 upon interaction with its C centre (Mode I, Fig. 2). This binding mode is generally observed in electron-rich metals, where electron transfer is facilitated by metal coordination with the electrophilic carbon centre. In this type of coordination with electron-rich metal ions, the LUMO of CO_2 gets populated, resulting in the re-hybridization of the C atom and a transformation in its geometry from linear to bent. The other mode of interaction involves one of the oxygen atoms with a metal ion generating the η^1–(O) binding mode (Mode II, Fig. 2). In this interaction, an electron-deficient metal ion binds with the nucleophilic 'O' centre of CO_2. The third type of interaction (Mode III, Fig. 2) corresponds to the bidentate binding mode, in which the metal ion functions as an ambiphilic centre coordinating in an η^2(C, O) fashion, where the metal ion binds with both the carbon and oxygen centres. Here, the metal ion acts in a synergistic fashion, in which a suitable metal orbital filled with electrons interacts with the C-centred LUMO, while the O-centred HOMO interacts with the empty d-orbital of the metal ion. Mode IV bonding represents the η^2 (O,O) bonding mode (Fig. 2), which is usually known as the "metal carboxylate" type of binding.

In this regard, it should be noted that catalytic processes involving CO_2 without a metal is challenging. Consequently, researchers assumed that CO_2 cannot be activated under metal-free conditions. However, recent developments have made it possible to overcome this challenge, where the transition metal-free activation of CO_2 has been demonstrated. The most prominent example of metal-free CO_2 activation can be cited from the nature itself, where an enzyme known as ribulose-1,5-bisphosphate carboxylase oxygenase (RuBisCO) can fix atmospheric CO_2 during photosynthesis.[23] The active site of the RuBisCO enzyme consists of the amino acid lysine, which is where the activation of CO_2 occurs. During this enzymatic process, the carbamate intermediate is formed through capture of CO_2 molecule by the nucleophilic amine group present in the active site of RuBisCO (Fig. 3). This understanding clearly highlights the affinity of the nitrogen lone pair of electrons to form an adduct with CO_2. During this interaction with the CO_2

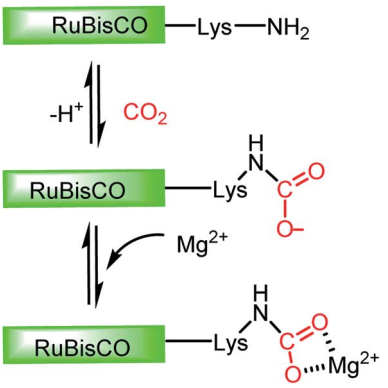

Fig. 3 Schematic representation of CO_2 activation in the active site of RuBisCo.

molecule, the electron density is transferred from the nitrogen to the low lying empty molecular orbital (LUMO) of CO_2, resulting in the bending of its linear structure in order to minimize the energy of the transition state. This nucleophilic interaction by the nitrogen of the amine group is similar to the metal binding Mode I, as mentioned in Fig. 2. Infact, the activation modes of CO_2 by metal ions can be considered as strategic guidelines for conceiving metal-free activation. To date, most of the metal-free activations follow the Mode 1- or Mode III-type interaction, as described in Fig. 2. However, this knowledge from nature clearly inspires the logical extension using various nitrogen bases for the activation of CO_2 as a viable route to replace the expensive and rare transition metals. To date, the reported metal-free activation of CO_2 can be divided into three distinct subclasses: (a) organic nucleophile-mediated activation (including nitrogen and phosphorus bases and N-heterocyclic carbenes (NHCs)); (b) ionic liquid (IL)-mediated activation and (c) ambiphilic activation by frustrated Lewis acid base pairs (FLPs). Organic nucleophiles are probably the most studied metal-free systems with regard to CO_2 activation owing to their availability and structural diversity, including alkyl/aryl mono- and polyamines, N-heterocyclic carbenes, amidine-like and guanidine-like derivatives. Among the organic bases, amidines and guanidines show better activity towards CO_2 activation. For example, 1,8-diazabicyclo[5.4.0]undec-7-ene (DBU) and 1,5,7-triazabicyclo[4.4.0]dec-5-ene (TBD) are the most recognised organic bases (Fig. 4), which are widely used in various transformations for the activation of the CO_2 molecule. The interaction between DBU and CO_2 molecule can be traced back to 1978 when Iwatani *et al.* reported the formation of a white solid upon the exposure of liquid DBU to CO_2 gas, which was characterized by IR spectroscopy and elemental analysis.[24] The high basicity of DBU is beneficial in the adduct formation with CO_2 by nucleophilic attack. In 2002, Franco and co-workers used this adduct for the synthesis of *N*-alkyl carbamates.[25] In 2004, Pérez *et al.* attempted to crystallize the DBU–CO_2 adduct by exposing a DBU solution in acetonitrile (ACN) to CO_2, but failed to isolate the desired crystals.[26] However, they were able to characterize the DBU–CO_2 adduct by NMR spectroscopy and the ^{13}C NMR spectrum in D_2O, which displayed a resonance at

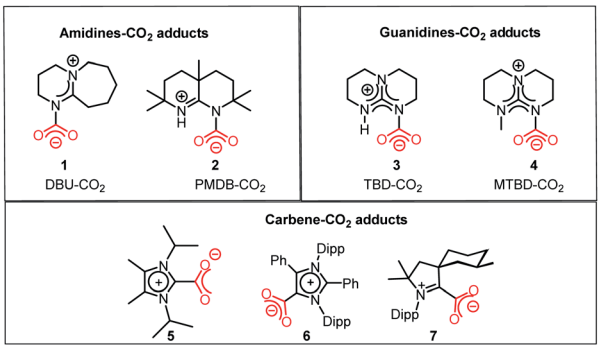

Fig. 4 Representative examples of isolated and well-characterized nitrogen base-CO_2 (**1–4**) adducts and NHC–CO_2 adducts (**5–7**).

δ 160.7 ppm. Up to 2010, the solid-state characterization of this nitrogen base-CO_2 adduct remained unsuccessful, until Villiers *et al.* first isolated the TBD–CO_2 adduct and characterised it *via* single crystal X-ray crystallography.[27] Dissolving TBD in anhydrous THF, and subsequent purging with CO_2 resulted in the formation of an off-white powder, which was crystallized at 70 °C under a CO_2 atmosphere. The N–C(CO_2) bond length was measured to be 1.48 Å, which is slightly longer than the typical N–C bond length (~1.35 Å) observed in various carbamates. The ^{13}C NMR spectrum recorded in CD_3CN revealed that the ^{13}C resonance arising from the CO_2 molecule displayed a downfield shift at δ 154.4 ppm. The reaction was carried out under anhydrous conditions in order to avoid the possible formation of bicarbonate. Subsequently, various nitrogen bases were used for the activation of CO_2. Some of the representative examples of these isolated adducts (**1–4**) are presented in Fig. 4.

In addition to nitrogen bases, N-heterocyclic carbenes (NHCs) emerged as another class of nucleophiles for the activation of CO_2. Soon after the isolation of the first NHC by Arduengo in 1991, NHC became the most versatile ligand for organometallic catalysis.[28] By virtue of their singlet ground state, the lone pair of electrons resides in a sp^2-hybridized orbital on the carbene carbon atom along with an unoccupied p orbital. The lone pair of electrons in the carbene centre makes NHCs nucleophilic, and hence they can act as very efficient σ donors. In 1999, Kuhn and co-workers first introduced NHCs to capture CO_2 molecules, where they demonstrated the formation of a zwitterionic adduct (**5**, Fig. 4) and characterised this adduct crystallographycally.[29a] Later in 2004, Louie and co-workers demonstrated the reversible binding of CO_2 with NHC, in which the addition of 1 atm CO_2 to 1,3-dimesitylimidazol-2-ylidene (IMes), or 1,3-bis(2,6-diisopropylphenyl)imidazol-2-ylidene (IPr) resulted in the formation of the corresponding zwitterionic imidazolium carboxylates.[29b] The IPr–CO_2 adduct was characterised *via* X-ray crystallography, and almost similar bond lengths of both C–O bonds in the adduct indicate that the negative charge is distributed equally. The ^{13}C NMR spectrum in CD_2Cl_2 showed a peak at δ 152.3 ppm, which was assigned to the ^{13}C resonance arising from the carboxylate group. Following this study, CO_2 adducts (**6** and **7**, Fig. 4) with various newer versions of NHCs such as abnormal NHC (aNHC)[30] and cyclic(alkyl)(amino) carbene (CAAC)[31] were isolated and characterized.

Another class of compounds commonly used for the activation of CO_2 molecules is ionic liquids (ILs). ILs are comprised of a cation and anion with one of the ions as an organic species possessing a delocalized charge. Ionic liquids exhibit high thermal stability and volatility, which can sustain both high temperature and pressure in the reaction medium, unlike organic solvents. Furthermore, the properties of ionic liquids can be tuned by varying the substituents on the organic part of the counterion, and hence they are often termed as "designer solvents". In 2002, Davis and co-workers reported the chemisorption of CO_2 on an amino group-functionalized IL.[32] In 2010, Lei and Dai developed anion-functionalized protic ionic liquids (PIL).[33] In their work, the PILs were formed *via* the combination of different super bases such as 7-methyl-1,5,7-triazabicyclo [4.4.0]dec-5-ene (MTBD) with partially fluorinated alcohols/imidazoles/phenols, *etc.* These strong bases have very high proton affinity, deprotonating even weak proton donors to form thermodynamically stable PILs. These PILs could capture CO_2 efficiently (**8**, Fig. 5). The nucleophilic character of ILs is exploited during the activation of CO_2, where the accumulated negative charge on the CO_2 molecule after its activation is stabilized by ion-pairing interactions with the cationic part of the IL, as shown in **8**. The major ILs used for the activation of CO_2 are depicted in Fig. 5.[33]

Another common mode of metal-free CO_2 activation is observed through frustrated Lewis pairs (FLPs). The concept of FLPs was developed from the initial observation by H. C. Brown in 1942 while studying the interaction between lutidine and BMe_3,[34] and later from the seminal work by Wittig and Benz,[35] Tochtermann,[36] Piers,[37] Oestreich[38] and many others. Based on the information gained through the years, FLPs are defined as a combination of a Lewis acid (LA) and Lewis base (LB) that is unable to form a classical acid–base adduct because of steric or geometric restrictions. The area of FLP research propelled in 2006 from the breakthrough made by Stephan and co-workers when $Mes_2P(C_6F_4)B(C_6F_5)_2$ was observed to reversibly bind with molecular hydrogen under mild reaction conditions.[39] The activation of H_2 was carried out using an FLP following the concept of synergistic

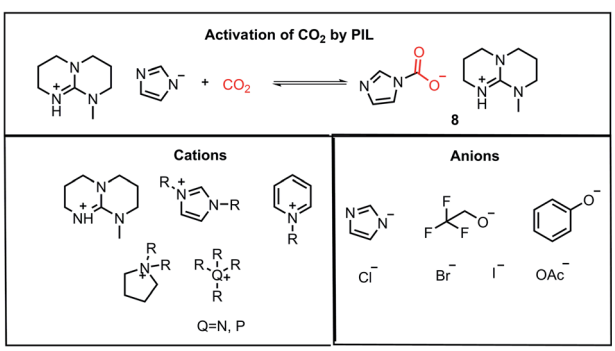

Fig. 5 Activation of CO_2 by PIL and combination of cations and anions for the construction of various ILs used for CO_2 activation.

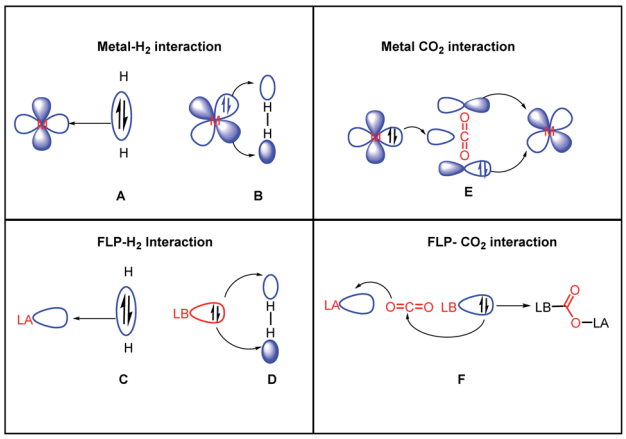

Fig. 6 Activation of H_2 and CO_2, highlighting the resemblance between transition metal-mediated activation and FLP-mediated activation.

activation, which is similar to the ambiphilic activation mode of a transition metal for a small molecule such as H_2. In the case of FLP-mediated activation, the electrons from the bonding orbitals of H_2 are transferred to the LUMO of the LA, while in the case of metal-mediated activation, the bonding electrons are transferred to a suitable empty d orbital (Fig. 6, **A** and **C**). Simultaneously, the electrons from the HOMO of the LB are transferred to the anti-bonding orbital of H_2, while in the case of metal-mediated activation, the d electrons are transferred to the anti-bonding orbital of the H_2 molecule which results in the cleavage of the H–H bond (Fig. 6, **B** and **D**). This concept was logically extended to the activation of CO_2 by FLPs. FLPs are capable of activating carbon dioxide since they are ambiphilic, allowing nucleophilic activation by the Lewis base (LB) at the carbon, and subsequent electrophilic activation by the Lewis acid (LA) at the oxygen atoms (Fig. 6, **F**). This bifunctional interaction was shown to be the key feature for the transition metal-mediated CO_2 activation process (Fig. 6, **E** and mode III, Fig. 2). The first report on FLP CO_2 activation appeared in 2009 by Stephen, Erker and co-workers, in which they reported a phosphino–borane LA–LB system for the formation of a zwitterionic product after activating the CO_2 molecule.[40] Specifically, $B(C_6F_5)_3$ and P^tBu_3 were added to bromobenzene under CO_2 atmosphere, which resulted in the formation of a white precipitate. It was found that the electrophilic C centre binds with the Lewis basic phosphorus unit, while the nucleophilic O of CO_2 binds with the Lewis acid boron, forming stable carboxylate adduct **9** (Scheme 1).

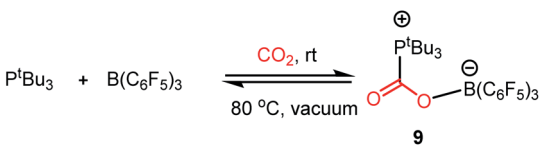

Scheme 1 Activation of CO_2 by P/B FLP, forming a carboxylate adduct.

3. Metal-free catalytic reduction of CO_2

The reduction of CO_2 to various value-added products leads to a decrease in the formal oxidation state of carbon centre of CO_2 is of great interest. CO_2 can be reduced sequentially to various energy intensive chemicals and fuels. For example, the 2e-, 4e-, 6e- and 8e-reduction of CO_2 can lead to the formation of formic acid, formaldehyde, methanol and methane, respectively (Scheme 2). Traditionally, these reductions have been carried out using transition metal-based catalysts.[41–43] In recent years, catalytic metal-free CO_2 reduction has emerged as an alternative to the expensive transition metal-mediated process. The previous section described various metal-free systems that can activate CO_2 under ambient conditions, opening up the possibility of the catalytic reduction of CO_2 under metal-free conditions.

3.1. Frustrated Lewis pairs for CO_2 reduction

Since the pioneering discovery in 2009 by Stephen, Erker and co-workers[40] on CO_2 activation by a phosphino–borane FLP system, CO_2 reduction has taken a quantum leap in the last decade. The first FLP-mediated CO_2 activation followed by its reduction into methanol was reported in 2009 by Ashley and O'Hare.[44] The reduction of CO_2 into methanol was accomplished using hydrogen gas in a stoichiometric amount. Their work took advantage of the fact that FLP can split the hydrogen molecule,[39] and subsequently the hydrogen activation is integrated with the CO_2 activation step to realize the thermodynamically challenging conversion. In this work, the combination of $B(C_6F_5)_3$ and TMP (TMP = 2,2,6,6-tetramethylpiperidine) in presence of H_2 and CO_2 resulted in the formation of a formatoborate complex, [TMPH]-[$HCO_2B(C_6F_5)_3$] (**11**), under heating (Scheme 3A). This observation can be explained considering stepwise activation of hydrogen and CO_2 molecules. The reaction between an equimolar amount of TMP and $B(C_6F_5)_3$ in the presence of H_2 yields [TMPH][$HB(C_6F_5)_3$] (**10**), where the H_2 molecule is heterolytically cleaved. This splitting of the hydrogen molecule by an FLP composed of TMP/$B(C_6F_5)_3$ was previously proposed by Sumerin *et al.*[45]

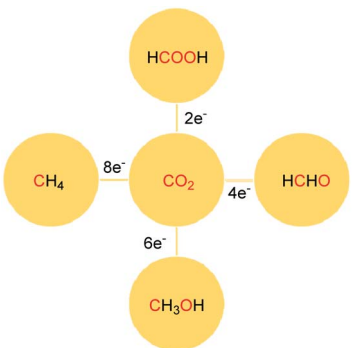

Scheme 2 Sequential reduction of CO_2 by 2e, 4e, 6e and 8e leads to the formation of various chemicals and fuels.

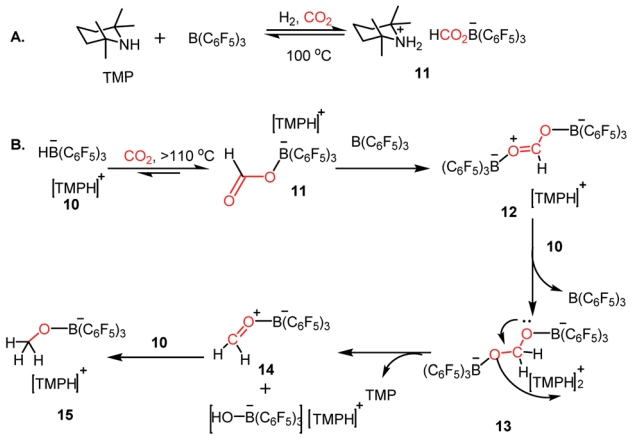

Scheme 3 (A) CO_2 activation in the presence of TMP/$B(C_6F_5)_3$/H_2. (B) Reduction of CO_2 with H_2 by FLP composed of TMP/$B(C_6F_5)_3$.

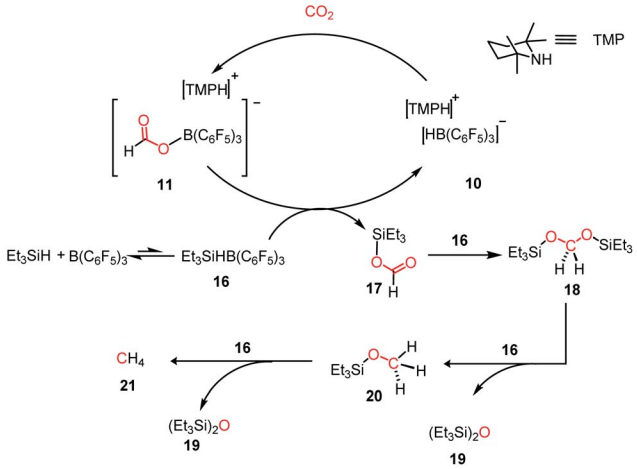

Scheme 4 Converting stoichiometric CO_2 reduction into catalytic process by adding excess $B(C_6F_5)_3$ and Et_3SiH to the TMP/$B(C_6F_5)_3$ system.

Subsequently, heating **10** in toluene above 110 °C under 1 atm CO_2 led to the formation of the formatoborate complex [TMPH][$HCO_2B(C_6F_5)_3$] (**11**, Scheme 3B). A carbonyl stretch at 1662 cm^{-1} was observed in the IR spectrum of complex **11** and the ^{13}C NMR spectrum revealed a resonance at δ 169.9 ppm, confirming the incorporation of CO_2. Furthermore, the structure of **11** was established by single crystal X-ray study. Finally, purging CO_2 in a mixture of TMP/$B(C_6F_5)_3$ in C_7D_8 under an H_2 atmosphere resulted in their quantitative conversion into [$CH_3OB(C_6F_5)_3$][TMPH] (**15**) after 6 days of heating at 160 °C. The formation of methanol in ~17–25% yield was observed after vacuum distillation. This may be explained considering following steps presented in Scheme 3B. Specifically, upon heating, **11** reversibly decomposes to **10**, which stays in equilibrium with TMP, $B(C_6F_5)_3$ and H_2. The free $B(C_6F_5)_3$ present in the medium can be arrested by the acyl oxygen of **11** to produce intermediate **12**. This activated formate intermediate **12** can be reduced by 1 equivalent of **10** to form acetal **13**, releasing $B(C_6F_5)_3$. Due to the instability of acetal in solution, the $[TMPH]^+$ counterion serves as the H^+ donor and **13** is converted into **14** and $[TMPH]^+[B(C_6F_5)_3OH]^-$. Next, **14** undergoes reduction in the presence of **10** in the medium to form **15**. The formation of methanol can be explained by considering the reaction of **15** with TMP or its conjugate acid. Even though this work represents the first reduction of CO_2 to methanol using an FLP-based system under a low pressure of CO_2 (1–2 atm), it suffers from a serious drawback since it is not a catalytic process. Thus, to address this shortcoming, Piers and coworkers reported that the addition of a hydrosilane to the reaction mixture in the presence of excess $B(C_6F_5)_3$ transforms the process into a catalytic one.[46] In the presence of excess $B(C_6F_5)_3$ and triethylsilane, the $B(C_6F_5)_3$/Et_3SiH adduct **16** is generated, which can rapidly hydrosilate the formatoborate complex **11** to form formatosilane compound **17**, regenerating $[TMPH]^+[HB(C_6F_5)_3]^-$ **10** (Scheme 4), thus making this process catalytic. Subsequently, the formatosilane **17** is further hydrosilated by **16** sequentially to $(Et_3SiO)_2CH_2$ (**18**), Et_3SiOCH_3 (**20**) and CH_4 (**21**), leaving $(Et_3Si)_2O$ (**19**) as a by-product.

Although, this reaction was catalytic, it still lacked good efficiency. The low efficiency was attributed to multiple factors such as the nature of the ion pair formed in the reaction medium[47] and the high entropy of the FLP system, as pointed by Fontaine and coworkers,[12,48] which originates from the use of discrete molecules of LA, LB and CO_2. Thus, to favour the reaction entropically, the LA and LB centres were assembled within the same molecule. In this regard, in 2013, an aryl bridged phosphine–borane system was introduced for the catalytic hydroboration of CO_2 into methoxyborane, which could further be hydrolysed to methanol.[48] In this work, the phosphine–borane 1-Bcat-2-PPh_2–C_6H_4 (cat = catechol) (**22**) functions as an ambiphilic system for the reduction of carbon dioxide in presence of various hydroboranes, resulting in the formation of CH_3OBR_2 or $(CH_3OBO)_3$ as the product. The TON (turnover numbers) and TOF (turnover frequencies) reported were as high as >2950 and 853 h^{-1}, respectively (Scheme 5A). In a typical catalytic run, exposing 1-Bcat-2-PPh_2–C_6H_4 to 1 atm of CO_2 at room temperature in the presence of 100 equiv. of HBcat resulted in the formation of a white precipitate. The white precipitate was characterized as catBOBcat. Analyzing the solution by ^1H NMR spectroscopy showed the presence of a new singlet at δ 3.37 ppm, which was attributed to CH_3OBcat. Moreover, this FLP reduced CO_2 in the presence of $BH_3 \cdot SMe_2$ at 70 °C with a TOF of 973 h^{-1} and TON of up to 2950, which is comparable to that of transition metal catalysts. This was the first report where BH_3 was introduced as a hydrogen source for the catalytic reduction of CO_2. A detailed DFT study was conducted to understand the mechanism of the reaction.[49] The reaction proceeds *via* a three-step process, in which CO_2 is first reduced to formatoborate, followed by formaldehyde, and then the final product methoxyborane (Scheme 5B). Four different modes of activation of borane were considered during this calculation and the most feasible one involved the simultaneous activation and binding of both borane and CO_2 to the catalyst (Scheme 5B). As the first step, the Lewis basic phosphorus atom present in the FLP activates the boron centre of the

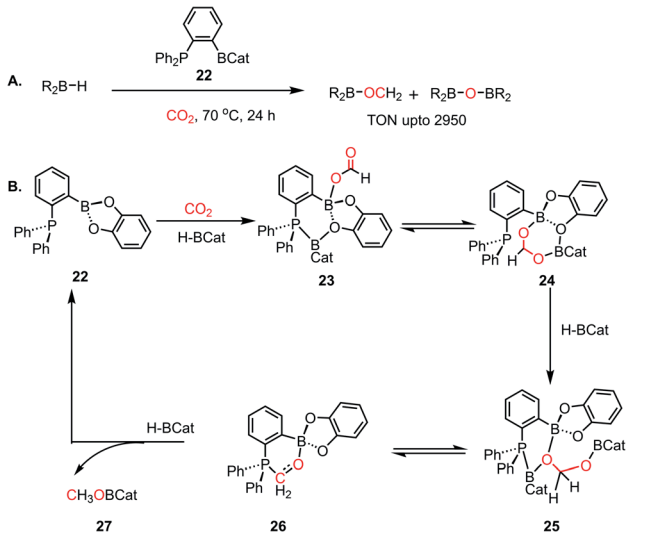

Scheme 5 (A) Catalytic reduction of CO_2 using ambiphilic B/P FLP catalyst. (B) Plausible catalytic cycle using ambiphilic B/P FLP catalyst based on DFT calculation.

hydroborane by forming an adduct, and the enhanced nucleophilicity of the borane causes hydride to transfer to the electrophilic carbon of CO_2, forming a formate anion. Further, the formate anion can bind with the boron centre of the catalyst in a concerted way, thus resulting in intermediate **23** (see Scheme 5B). However, this type of activation contradicts the classical FLP-mediated CO_2 activation. This simultaneous activation results in a four-coordinated boron centre observed in **23**, which can stay in equilibrium with compound **24**. The next step involves the formation of formaldehyde intermediate **26** (Scheme 5B) upon reduction by hydroborane through intermediate **25** (see Scheme 5B). In the next step, in the presence of hydroborane, **26** is further reduced to the corresponding methoxyborane (**27**), while regenerating the catalyst **22**. In subsequent study with ^{13}C labeled CO_2,[50] it was identified that **26** plays the role of an active catalyst instead of a reaction intermediate, as portrayed in Scheme 5B. The ambiphilic nature of the catalyst where LA–LB is present in the same molecule plays a key role in the efficacy of this FLP-based catalyst.

In 2014, Stephan's group reported an intermolecular P/B-based FLP for the catalytic reduction of CO_2 (Scheme 6A).[51] In their report, a stoichiometric reaction between 9-BBN, phosphine (R_3P; R = ^{t}Bu, 4-MeC_6H_4) and CO_2 yielded (R_3PCH_2-O)(HC(O)O)B(C_8H_{14}) (**28**) (see Scheme 6B), in which CO_2 is incorporated both in the form of formate and a phosphonium methoxy unit, and its structure was characterized by X-ray crystallography. This control experiment established the CO_2 activation step using the P/B FLP. This observation prompted them to extend their study in a catalytic direction, where in the presence of a catalytic amount of ^{t}Bu$_3$P, CO_2 was successfully reduced using 9-BBN at 60 °C to methoxyborane with the highest TON of 5500 (Scheme 6A). When the catalytic reaction was performed in the presence of 9-BBN, 4 mol% ^{t}Bu$_3$P, using CO_2, it yielded various reduction intermediates. The first step involves the formation of a boron formate intermediate **30** *via*

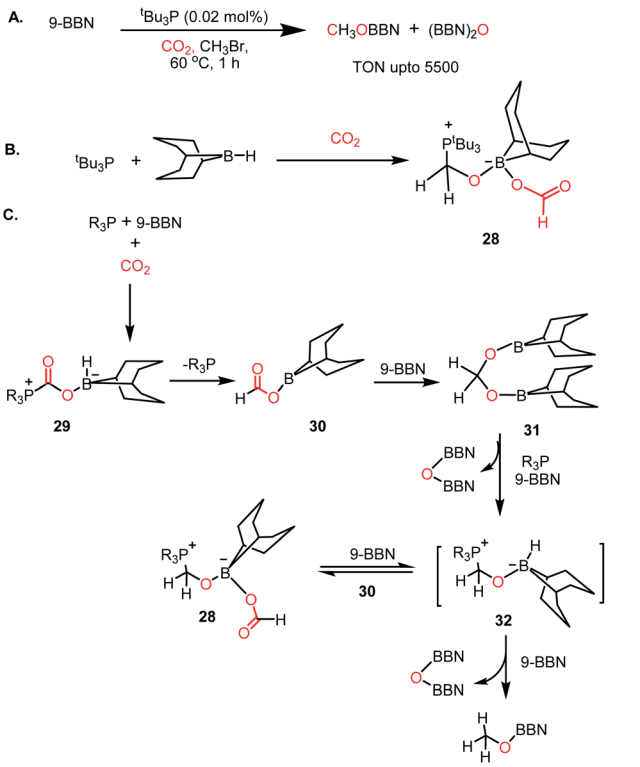

Scheme 6 (A) Intermolecular B/P FLP for the catalytic reduction of CO_2. (B) Activation of CO_2 by B/P FLP. (C) Plausible mechanistic cycle for B/P FLP-mediated CO_2 reduction.

intermediate **29**, which is then converted into diolate derivative **31** (Scheme 6C). Subsequently, **31** can further react with R_3P *via* the elimination of a B–O–B dimer to generate compound **32**. Compound **32** can react with boron formate **30** to generate compound **28**, which was characterized *via* X-ray crystallography, or it can be further reduced to methoxyborane by reaction with 9-BBN (Scheme 6C).

In 2012, Stephan's group reported an adduct of NHC with 9-borabicyclo[3.3.1]nonane (9-BBN) in the presence of P^{t}Bu$_3$, which could be used for the activation of H_2.[52] Inspired by this work, the same group introduced an intramolecular FLP by reacting a phosphine-bearing NHC derivative with 9-BBN. The reaction proceeds through C–N bond cleavage of NHC and insertion into the B–C bond of 9-BBN resulting in ring expansion (**33**, Scheme 7A).[53] This adduct consists of a strong basic site (P center) and weak Lewis acidic site (B center), making it a suitable intramolecular FLP, **33**. This FLP was used for the

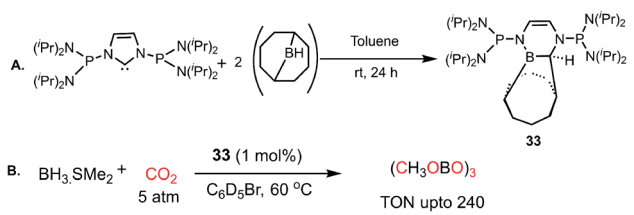

Scheme 7 (A) Preparation of intramolecular P/B FLP system. (B) Catalytic CO_2 reduction using the P/B FLP **33**.

catalytic hydroboration of CO_2 in the presence of a boron hydride (Scheme 7B), exhibiting a TON of 240 and affording methoxyborane.

In 2016, Cantat and co-workers introduced another class of FLPs, in which a nitrogen-stabilized silylium cation was used for the activation of CO_2.[54] It should be noted that being isoelectronic with boranes, silyl cations are considered as a good replacement for boranes as Lewis acids. A series of base-stabilized silylium species was prepared, which formed an N/Si FLP–CO_2 adduct (**34**) upon exposure to CO_2. This adduct with CO_2 was characterized by X-ray study. These silicon species were found to be active catalysts in the hydroboration of CO_2 to methoxyborane with various boranes, giving the highest TOF of 3.7 h^{-1} (Scheme 8). In these FLPs, the silicon centre exhibits affinity towards oxygen, while the N center binds with the C of CO_2 during the activation process.

In 2018, the viability of commercially available alkylic carbodiimides (CDIs) was demonstrated when they were treated with boranes such as 9-BBN or BH_3 in the catalytic hydroboration of CO_2.[55] The catalytically-active FLP species were formed *in situ via* the reaction of CDIs with borane and CO_2. The CDIs react with boron hydrides to form boron amidinates,[56] which have potential to act as an FLP owing to the presence of N/B combinations. Commercially available diisopropylcarbodiimide (CDI, **35**) was used as a catalyst for reduction of CO_2 using various hydride sources such as 9-BBN and $BH_3 \cdot SMe_2$ under mild conditions (1 atm CO_2, 25–60 °C) to give a mixture of methoxyborane and bis(boryl)acetal (Scheme 9A). Various stoichiometric reactions were carried out to elucidate the reaction mechanism, and it was proposed that the first step involves the hydroboration of **35** by borane to yield boron amidinate (**36**), which further reacts with CO_2 to form a 1,2 addition intermediate (**37**), as shown in Scheme 9B. Further reaction with another unit of 9-BBN led to the formation of a formaldehyde adduct (**38**). All these intermediates (**36–38**) were identified and characterized *via* X-ray crystallography. Complex **38** was identified as the active catalyst, which reduces CO_2 to methoxyborane and bis(boryl)acetal upon the sequential addition of 9-BBN. It may be noted that in the case of $BH_3 \cdot SMe_2$, the products of CO_2 reduction are $(OBOMe)_3$ and $B(OMe)_3$ (Scheme 9A).

Thus far, we have discussed CO_2 reduction using various FLP-based catalysts in presence of hydrosilane or hydroborane as a reducing agent. Although these processes exhibit good catalytic efficacy, there is always room for further improvement since these reducing agents are expensive. In this regard, H_2 gas, owing to its low cost, can be a good replacement for the expensive silane/borane reagent. Consequently, the development of metal-free systems that can activate both CO_2 and H_2 simultaneously and selectively is highly rewarding, although very challenging. In 2015, Stephan and Fontaine *et al.* introduced an intramolecular B/N-based FLP, where CO_2 was reduced to formates, acetals and methoxides in the presence of molecular H_2 (Scheme 10A).[57] An ambiphilic B/N FLP **39** was developed, which upon exposure to H_2 gas at 80 °C resulted in the formation of **40** (Scheme 10B) with the sequential elimination of mesitylene, which was evident from the ^1H NMR spectroscopy of the reaction mixture. This observation suggests the possibility of a protodeborylation process as a result of H_2 activation. Further, compound **40** generated upon H_2 activation can act in dual fashion for the activation of CO_2 together with its reduction. For example, **40** can act as an ambiphilic FLP for CO_2 capture, and subsequently the BH_2 group present in **40** may function as a reducing agent. Although the selectivity of the process is somewhat compromised, resulting in a mixture of products, this result suggests that an appropriate strategy in designing FLPs can provide an avenue for the design of metal-

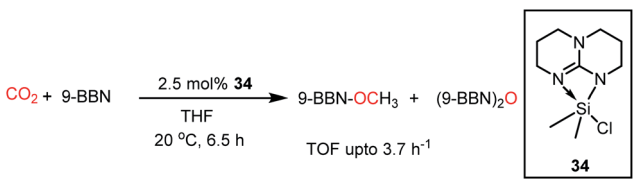

Scheme 8 Reduction of CO_2 using N/Si FLP system **34**.

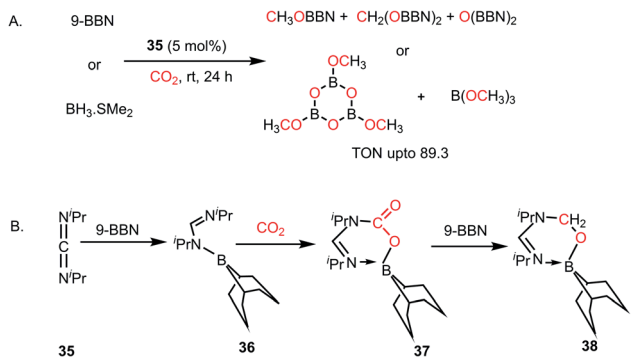

Scheme 9 (A) Catalytic reduction of CO_2 using CDI, forming *in situ* FLP, which acts as a catalyst. (B) Formation of the active catalyst **38** for CO_2 reduction using CDI.

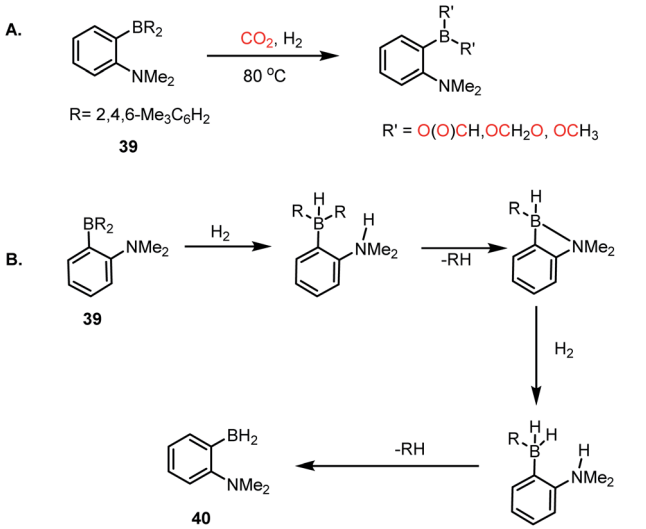

Scheme 10 (A) CO_2 reduction in the presence of a B/N FLP using molecular H_2. (B) Heterolytic cleavage of H_2 in the presence of a B/N FLP, resulting in **40**.

free catalysts for H_2/CO_2 chemistry. Accordingly, this work represents a unique way where H_2 was used as a reductant for the reduction of CO_2, avoiding borane/silane as reductant.

3.2 NHC mediated CO_2 reduction

As mentioned earlier, N-heterocyclic carbenes (NHCs), owing to their strong nucleophilicity, are known to form imidazolium carboxylates upon reaction with CO_2,[29] which was explored towards the catalytic reduction of CO_2 to form various value-added products. In 2009, Ying and co-workers first reported the hydrosilylation of CO_2 in the presence of an NHC to form methanol under ambient conditions.[58] This was the first time a metal-free system was involved in the catalytic reduction of CO_2 to methanol. It was observed that the 1,3-bis(2,4,6-trimethylphenyl)imidazolium carboxylate (**41**) under a CO_2 atmosphere resulted in the hydrosilylation of CO_2 by diphenylsilane at room temperature within 6 h (Scheme 11A). ^{1}H NMR spectroscopy and GC-MS studies identified the presence of diphenylformoxysilane, diphenyldiformoxysilane, bis(silyl) acetal and silylmethoxide in the reaction mixture, which gave insight into the mechanistic pathway of this fascinating conversion. A peak at δ 3.5 ppm in the ^{1}H NMR spectrum of the reaction mixture in DMF-d_7 confirmed the formation of silyl methoxide, which can be easily hydrolysed to methanol. To understand the reaction mechanism, various control reactions were carried out using isotopically labelled $^{13}CO_2$ gas. The ^{13}C $\{^1$H$\}$ NMR spectroscopic studies revealed the appearance of new peaks at around δ 160 ppm, indicating the formation of formoxy and di-formoxy silane. The peak at δ 85 ppm was ascribed to the silyl acetal group and the resonance at δ 50 ppm was assigned to silyl methoxide. During the course of the reaction, the resonance at δ 85 ppm diminished together with an increase in the intensity of the peak at δ 50 ppm, indicating the conversion of acetals into methoxide. This catalytic conversion led to the highest TON of 1850 and TOF of 25.5 h^{-1} under ambient conditions (Scheme 11A). Finally, treatment of the reduced products with $NaOH/H_2O$ produced methanol. The detailed mechanistic understanding remained unclear; however, a plausible cycle was proposed, in which imidazolium carboxylate **41** first attacks the silicone centre of diphenylsilane, which facilitates the hydride transfer in a concerted manner producing formoxysilane **42** (Scheme 11B). This releases a free NHC, which captures CO_2 to regenerate **41**. Formoxysilane **42** can be reduced by hydrosilanes to form the silyl methoxide and the reduction continues until all the hydrosilanes are consumed (Scheme 11B). This mechanistic proposal later attracted considerable attention when Wang and co-workers came up with a detailed mechanistic proposal based on DFT calculations.[59] In their study, it was shown that the first step involves the activation of the Si–H of silane by NHC, which results in the transfer of hydride to the electrophilic carbon centre of CO_2 to form a formate ion. Based on their calculations, the prior activation of the carbon centre of CO_2 by NHC coordination was found to be energetically less favourable than silane activation. Further reduction of formate by additional equivalents of silane resulted in the formation of methoxyborane. They proposed a mechanistic path, where NHC directly coordinates to the silane centre instead of CO_2. However, Zhang and co-workers further came up with a detailed study to reveal the underlying mechanism.[60] The stoichiometric reaction performed between NHC and silane did not show any change in chemical shift values, even after prolonging the reaction for 2 weeks. Hence the possibility of NHC coordination to silane was discarded. In their study, it was uncovered that the reaction takes place through a three-step cascade pathway. The first step of the cascade mechanism involves the interaction of diphenylsilane with imidazolium carboxylate **41** under a CO_2 atmosphere to form a formoxysilane intermediate (**42**, Scheme 11C) *via* a five-membered transition state **43**. This step represents the rate-limiting step since it possesses the highest energy barrier. The next step proceeds with the hydride transfer from diphenylsilane to the formoxysilane intermediate and the formation of bis(silyl)acetal (**44**, Scheme 11C), whereas the third step involves the formation of the methoxy silane product by reacting with another molecule of silane, while eliminating silyl ether (Scheme 11C).

The efficiency of NHC in the reduction of CO_2 prompted the use of an abnormal NHC (aNHC), exhibiting superior nucleophilicity over normal NHC.[30] As mentioned in the previous section, the synthesis of the aNHC–CO_2 adduct (**6**) was reported by Bertrand and co-workers in 2009.[30] Later, the introduction of this adduct in synthesis of methanol was carried out by Mandal and co-workers in 2016 *via* the hydroborylative reduction of CO_2.[61] The use of an abnormal N-heterocyclic carbene and corresponding CO_2 adduct was reported for the reduction of CO_2 to methoxyborane under ambient conditions (1 atm CO_2, rt) using various hydride donors such as 9-BBN, HBPin, CatBH,

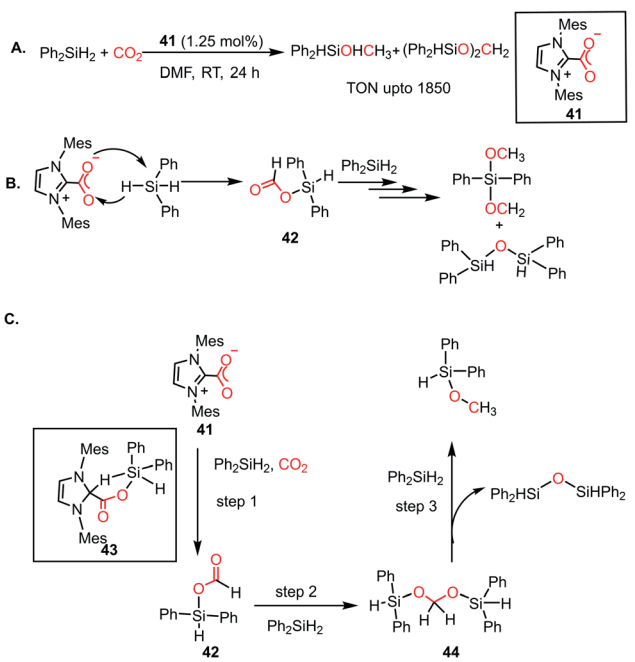

Scheme 11 (A) Hydrosilylation of CO_2 using NHC as a metal-free catalyst. (B) Reduction of CO_2 to methoxide in the presence of NHC carboxylate **41**. (C) Three-step cascade pathway for the reduction of CO_2 using NHC-carboxylate **41**.

$BH_3 \cdot SMe_2$ and $BH_3 \cdot THF$. The stoichiometric reaction between the *a*NHC–CO_2 adduct and 9-BBN under a CO_2 atmosphere resulted in the formation of a colourless solution, which was identified as a boron diformate (**47**), as established by various spectroscopic studies, and finally its solid-state structure was determined by X-ray crystallography. The ^{1}H NMR spectrum showed two singlets at δ 8.51 and 8.33 ppm with a 2 : 1 intensity, which corresponds to formate and C5–H of *a*NHC, respectively. The reduction of CO_2 was performed in the presence of 9-BBN using **47** as a catalyst, leading to a TON of 6000, which is among the highest TON reported using a metal-free catalyst under ambient conditions (Scheme 12A). Based on a series of control experiments together with DFT studies, the mechanistic cycle was proposed, in which *a*NHC–CO_2 (**6**) upon reaction with 9-BBN forms adduct **45**, activating the B–H bond of borane. Subsequently, **45** further undergoes an insertion reaction with CO_2, which results in the formation of a four-coordinated boron species **46**. The addition of two molecules of 9-BBN to **46** results in the formation of a zwitterionic borondiformate **47** together with the release of a B–O–B dimer. Subsequently, another molecule of 9-BBN reacts with **47**, which results in the regeneration of **45** together with the formation of a methoxide derivative (Scheme 12B).

However, all these catalytic systems reported thus far demand commercially available, often greater than 99.99% pure CO_2, which is available from a cylinder, to carry out the reduction. Hence, the development of catalytic systems that can capture CO_2 from the air and perform the reduction is of great interest. In 2019, Mandal and co-workers reported the use of an abnormal N-heterocyclic carbene borane adduct (**49**) obtained from aNHC **48** by reacting it with 9-BBN to capture atmospheric CO_2, and its reduction into formic acid and methanol under ambient conditions (Scheme 13A).[62] Upon the exposure of adduct **49** in benzene-d_6 to air overnight, it showed a sharp colour change from light yellow to green. ^{1}H NMR spectroscopic analysis of the new compound showed two singlets at δ 8.53 and 8.55 ppm with the equal intensity, which were attributed to the formate anion and C5–H of the aNHC moiety, respectively indicating formation of **50**. ^{13}C NMR spectroscopic studies also supported the presence of a formate group, which is evident from the appearance of a resonance at δ 169.2 ppm. This observation clearly indicates the activation of atmospheric CO_2. The ^{11}B NMR spectrum of **50** showed a singlet at δ 20.8 ppm, supporting the presence of free boric acid, which was observed in the crystal lattice of **50** (Scheme 13A). The formation of boric acid may be attributed to hydrolysis of 9-BBN by the moisture present in air with the elimination of a cyclooctane molecule. X-ray studies illustrated that the exposure of CO_2 to adduct **49** led to the incorporation of CO_2 as a formate anion, resulting in the formation of **50** (Scheme 13A). Upon further treatment with NaOH solution, **50** formed sodium formate. On the other hand, in the presence of air, this aNHC–BBN adduct **50** underwent reduction with 10 equivalents of 9-BBN to form boronmethoxide together with the release of H_2 gas (Scheme 13B). This

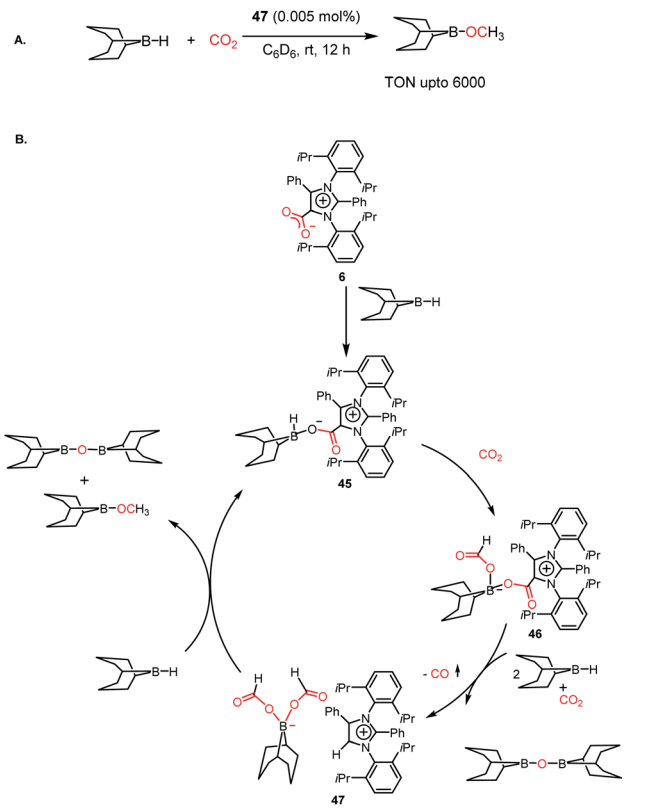

Scheme 12 (A) Catalytic reduction of CO_2 in the presence of aNHC borondiformate **47**. (B) Plausible mechanistic cycle for the reduction of CO_2 using aNHC.

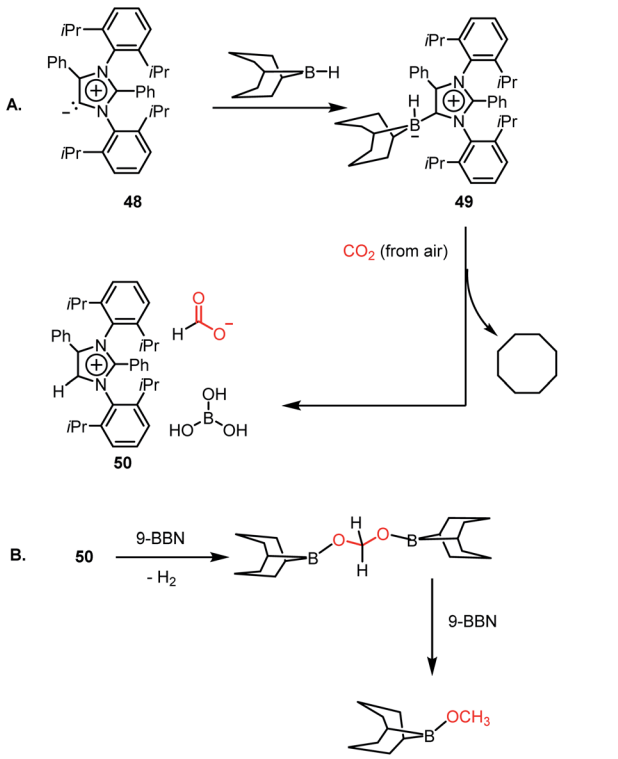

Scheme 13 Capture of CO_2 from the air under ambient conditions by aNHC–BBN adduct **49** and its reduction to formate (A) and methoxide (B).

work represents the first metal-free system where CO_2 is captured from the air under a low concentration of CO_2 (~400 ppm) and further reduced to formate or methoxide.

3.3. CO_2 reduction by various other metal-free catalysts

Besides FLP- and NHC-mediated conversion, several other methods have been reported for the metal-free reduction of CO_2. Among them, nitrogen bases are known for the catalytic reduction of CO_2 into methoxyborane in the presence of a hydroborane. In 2014, Cantat and co-workers introduced TBD, Me-TBD (MTBD) and DBU and other nitrogen bases for the metal-free reduction of CO_2 in the presence of 9-BBN or CatBH at room temperature to achieve a TON of up to 648 (Scheme 14A).[63] NMR spectrometric monitoring of the reaction mixture revealed that over time, CO_2 is reduced to borylformate, which undergoes further reduction to acetal, and subsequently to methoxyborane. For long time, TBD has been known to activate CO_2, which forms a TBD–CO_2 (**3**) adduct.[27] Hence, the formation of the TBD–CO_2 adduct is expected to be the first step in the reduction cycle. The stoichiometric reaction between **3** and 9-BBN in THF resulted in the formation of an adduct **51** together with other reduced products (Scheme 14B). X-ray study of **51** showed that the acidic NH proton of **3** is replaced with a dehydrido 9-BBN unit. **51** can be considered an intramolecular N/B FLP system captured with a CO_2 molecule. Based on further control reactions, a plausible scheme was proposed, in which the CO_2 molecule in **51** acts a Lewis base and coordinates with hydroborane to form adduct **52**, which in turn facilitates the hydride transfer from borane to carbon, forming **53**. In the presence of CO_2, **53** is regenerates to **51**, leaving boron formate, which is further reduced to methoxyborane. In the case of MTBD, it was found that the reaction proceeds with the activation of borane, followed by the incorporation of CO_2.

Similar to nitrogen bases, a carbanion such as *N*-methyl-4,5-diazafluorenide (**54**) was used for the catalytic reduction of CO_2 by Song and co-workers.[64] The reaction between **54** and CO_2 resulted in the formation of a carboxylic acid adduct (**55**) (Scheme 15). The carboxylic acid proton of **55** showed a resonance at δ 11.02 ppm in DMSO-d_6, whereas the ^{13}C NMR spectrum showed a resonance at δ 166.4 ppm attributable to the carbon of CO_2. The reduction of CO_2 with various hydroboranes such as HBPin, 9-BBN, $BH_3{\cdot}SMe_2$, and HBCat in the presence of 1 mol% **54** resulted in the formation of the corresponding methoxyboranes (Scheme 15A). In this case, the catalytic activity originates from the charged carbanionic form, which is actually in resonance with the uncharged form. The charged species can interact with the CO_2 molecule by forming an adduct. To avoid the contribution from the uncharged form of resonance, the same group introduced zwitterionic complex **56** (Scheme 15B).[65] Upon treatment of **56** with 1 atm CO_2 under ambient conditions, an immediate colour change was observed, and the product was confirmed to be the CO_2 adduct (**57**) by X-ray crystallography. The catalyst efficiently performed hydroboration of CO_2 using 9-BBN or $BH_3{\cdot}SMe_2$ under ambient conditions, resulting in a TON of 281 (Scheme 15B).

In addition to nucleophiles, electrophilic reagents such as Lewis acids also can act as catalysts for CO_2 reduction. For example, in 2016, Okuda and co-workers reported the use of a weak Lewis acid BPh_3 for the selective hydrosilylation of CO_2 to silyl formate.[66] It should be noted that the selective reduction to silyl formate is a challenging task owing to the affinity of carbonyls to undergo over reduction. In the presence of $PhMeSiH_2$ and 10 mol% BPh_3 n acetonitrile, CO_2 was selectively hydrosilylated to $PhMeSiH(O_2CH)$ at 40 °C (Scheme 16). It was proposed that BPh_3 plays a dual role in this catalytic process, where it activates the hydride of silane by hydrogen bonding with the electrophilic boron centre. BPh_3 also can activate CO_2 by interaction between the B of BPh_3 and O of CO_2 (Scheme 16). This report highlighted that weaker non-fluorinated borane was efficient for the catalytic reduction of CO_2 into formate, opening the possibility of using Lewis acid-based catalysts.

In 2018, Wegner and co-workers introduced the concept of using a bidentate bis(borane) for the catalytic reduction of CO_2 into methane and methanol.[67] The presence of two oxygen

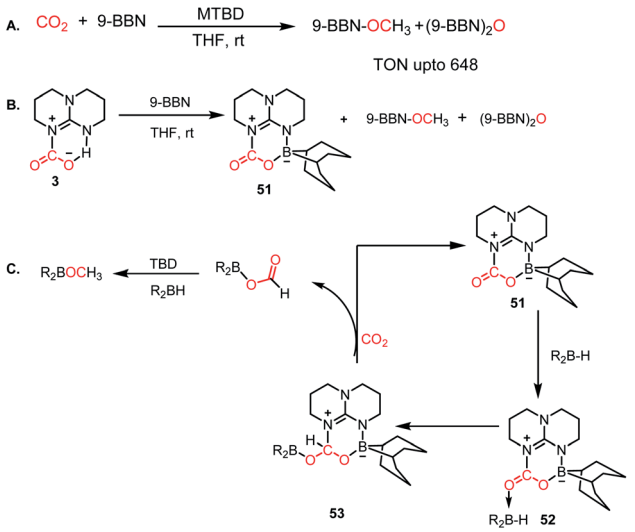

Scheme 14 (A) Catalytic CO_2 reduction by MTBD. (B) Formation of TBD–CO_2–BBN adduct **51**. (C) Plausible mechanistic cycle.

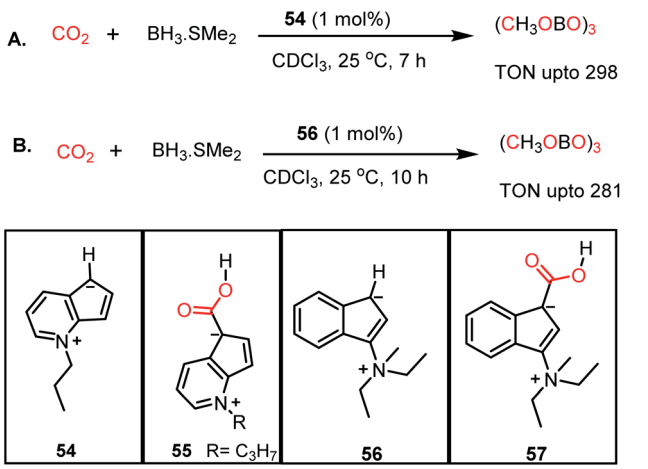

Scheme 15 Catalytic reduction of CO_2 using a carbanions; (A) **54** and (B) **56**.

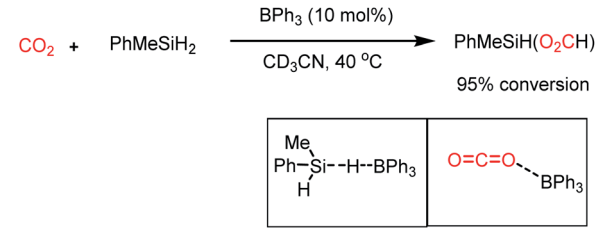

Scheme 16 Selective hydrosilylation of CO_2 into silylformate using a Lewis acid (BPh_3) as the catalyst.

atoms in CO_2 favours a bidentate mode of binding to the pair of intramolecularly integrated boron centres (Scheme 17A). Lithium *o*-phenylbisborate (**58**) was used as a catalyst in the presence of triethylsilane and $B(C_6F_5)_3$ to reduce CO_2 into a mixture of CH_4, $(Et_3SiO)_2CH_2$ and Et_3SiOMe (Scheme 17B). The presence of CH_4 was confirmed by the singlet at δ 0.14 ppm *via* ^{1}H NMR spectroscopy. The necessity of the bisborane catalyst was judged by a control reaction, which was performed using the monoborohyride $LiPhBH_3$, leading to a dramatic reduction in the efficiency. The reaction was selective towards methanol when the reducing agent was changed to HBpin instead of silane. Based on various control experiments, a plausible mechanism was proposed (Scheme 17C). Catalyst **58** reacts with CO_2 to form a precipitate, the NMR spectroscopic characterization of which was not possible because of its poor solubility. However, the IR spectroscopic analysis showed a strong absorption at 1592 cm^{-1}, which accounts for the presence of the C=O group, suggesting the formation of a CO_2 adduct with the catalyst. The next step involves intramolecular hydride transfer to generate formate **59** (Scheme 17C). This can further be reduced by the second BH_3 group of **59** to form acetal

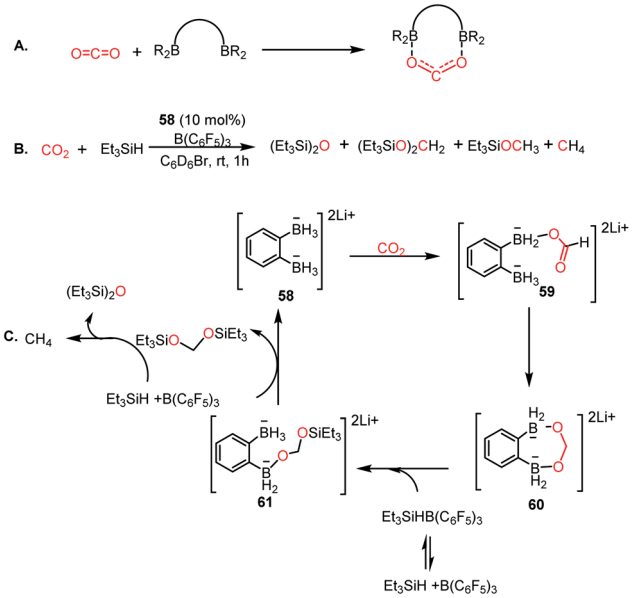

Scheme 17 (A) Activation of CO_2 using bidentate binding mode. (B) Catalytic reduction of CO_2 using a bis-boronhydride ligand in the presence of a silane. (C) Plausible mechanistic cycle for the reduction of CO_2.

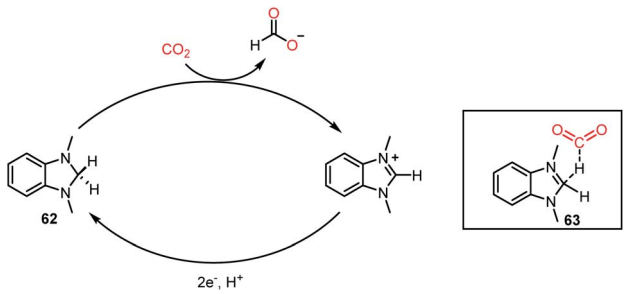

Scheme 18 Activation of CO_2 by an organic hydride donor.

60 (Scheme 17C). Next, the silane cleaves the acetal to form a disilylacetal (Scheme 17C) *via* intermediate **61**, which in turn can be reduced to methane.

Recently, a different class of catalysts was introduced by Lim, Musgrave and co-workers, where a benzimidazole hydride was used for the activation and reduction of CO_2.[68] Thus far, a sacrificial reductant together with a catalyst was mandatory to carry out the reduction of CO_2. In sharp contrast, an organic hydride donor was used to reduce CO_2 to $HCOO^-$, and the organic hydride donor could be regenerated *via* an electrochemical method, opening the possibility to act as a reductant and catalyst simultaneously. Organic hydrides can chemically reduce CO_2 to $HCOO^-$, but these reactions are limited to a stoichiometric version because of the limitation in regenerating the active catalyst. Interestingly, here, this challenge was addressed *via* an electrochemical method using metal electrodes. The reaction was performed using catalyst **62** in the presence of 20 psig of CO_2, and KBF_4 in DMSO-d_6 at 50 °C for 18 h, resulting in 66% yield of formate (Scheme 18). It was anticipated from DFT calculations that the interaction between CO_2 and hydride occurs through transition state **63**. The presence of salts provides a suitable polar environment to stabilize the ionic products and shifts the equilibrium towards product formation. This report represented the first approach where an organic hydride donor was used in the reduction of CO_2 to formate and integrated in the catalytic cycle by regenerating the active catalyst with the help of electrochemistry. Besides the catalytic systems described above, the reduction of CO_2 has been performed using various other catalysts such as phosphazene,[69] $NaBH_4$,[70] carbenoid compound,[71] and formamidinates.[72]

4. Metal-free reductive functionalization of CO_2

In addition to the reduction of CO_2 into formic acid, methanol and methane, the utilization of CO_2 may find application by undergoing reduction together with functionalization by forming new C–N bonds. As it is known, the major products of CO_2 functionalization without formal reduction include urea, polycarbonates, and salicylic acid. However, since the functionalization of CO_2 does not require any formal reduction in the carbon centre, energy storage cannot be achieved efficiently. Thus, to maintain energy economy, Cantat and co-workers introduced a diagonal approach, in which CO_2 undergoes

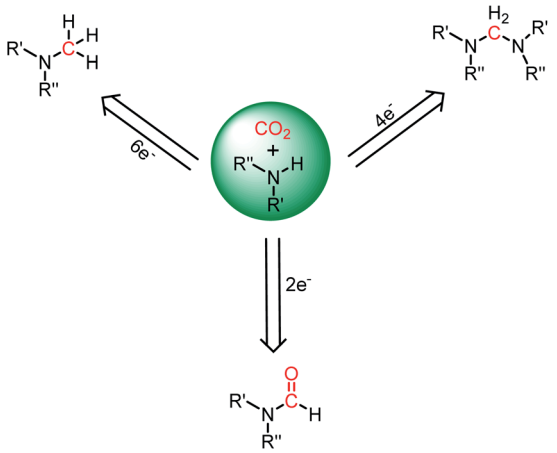

Scheme 19 Reductive functionalization of CO_2 with amines.

simultaneous reduction and functionalization in the presence of a reducing agent and functionalizing reagent to form a new C–N bond.[73] The major type of reductive functionalization involves the reduction of CO_2 in the presence of an amine to synthesize various energy storage materials such as formamides, aminals and methylamines, which are the 2-, 4-, and 6-electron reduced products of CO_2, respectively (Scheme 19). It is worth to mentioning that the synthesis of formamides *via* the reduction of CO_2 in the presence of amines was achieved by Vaska and co-workers in 1988.[74] Subsequently, various metal-free catalysts such as nitrogen bases, NHC, FLP, IL and others were introduced for this reductive functionalization of CO_2, and the following sections describe these developments.

4.1 Formylation of amines using CO_2

The formylation of amines using CO_2 produces formamides. Formamides represent the 2e-reduction products of CO_2 together with the formation of a new C–N bond, which are considered as one of the primary building blocks in organic synthesis. Traditionally, formamides are often synthesized from carbon monoxide under harsh reaction conditions.[75] The use of CO can be effectively replaced by CO_2 together with an appropriate reducing agent. In this regard, various transition metal catalysts have emerged using H_2 as a reductant. However, the harsh reaction conditions and poor selectivity with the use of H_2 as a reductant prompted the use of hydrosilanes as a milder alternative owing to their similar reduction potential.[76] In addition, the use of efficient metal-free catalysts with mild reaction conditions is preferable over expensive transition metals. The last decade has witnessed the development of efficient metal-free catalysts for the formylation of amines using CO_2, which are described herein. In 2012, Cantat and co-workers introduced TBD for the first metal-free catalytic reductive formylation of amines using a silane and CO_2.[73] Their preliminary computational study indicated that to carry out the functionalization of CO_2 using silanes, a functionalizing group (such as morpholine) with greater affinity towards carbon and less affinity towards silicon is required. The reaction between a secondary amine such as morpholine and TBD–CO_2 (**3**) in the presence of diethyl ether results in the formation of a hydrogen-bonded carbamate (**64**, Scheme 20A), in which CO_2 is transferred from TBD to morpholine, as confirmed by X-ray crystallography. Further, the reaction was performed using carbamate **64** and three equivalents of $(EtO)_3SiH$ in THF, which resulted in the reduction of the carbon centre to form the corresponding formamide together with the formation of **65** (Scheme 20B). This result represents the first report on the reduction of carbamates using silane as a reducing agent. Here, silicon plays a dual role, in which it promotes the reduction of the carbon centre and facilitates the cleavage of the C–O bond of CO_2. Subsequently, to develop a catalytic strategy for the reductive functionalization of amines, a series of control reactions was performed. Initially, different nitrogen bases such as TBD, MTBD, DBU, DABCO and DMAP were screened, where TBD exhibited the highest catalyitc efficiency. It was found that solvent-free conditions showed better activity. In the presence of 5 mol% TBD, CO_2 and $PhSiH_3$, morpholine was completely consumed to produce *N*-formylmorpholine at 100 °C in 24 h. Using the optimized reaction conditions, various amines underwent reductive formylation, which include aromatic and aliphatic amines to give up to 65% yield (Scheme 20C). This work represents the first report on the reductive functionalization of amines using CO_2 under metal-free conditions. However, this system is specific to amines and high temperature (100 °C) is needed since TBD is not nucleophilic enough to activate organic silanes. This drawback was addressed by introducing a stronger nucleophilic NHC for the formylation of amines.[77] Among the various NHC catalysts screened (IPr, IMes, s-IPr, s-IMes, Cl_2-IPr and I^{t}Bu), IPr (**66**) showed the highest reactivity, which was over 2000 times greater than that for the formylation of morpholine using TBD, CO_2, and $PhSiH_3$ at rt (Scheme 21). The scope of the formylation of various amines was tested using the optimized reaction conditions, and it was observed that the reaction proceeded smoothly for primary and

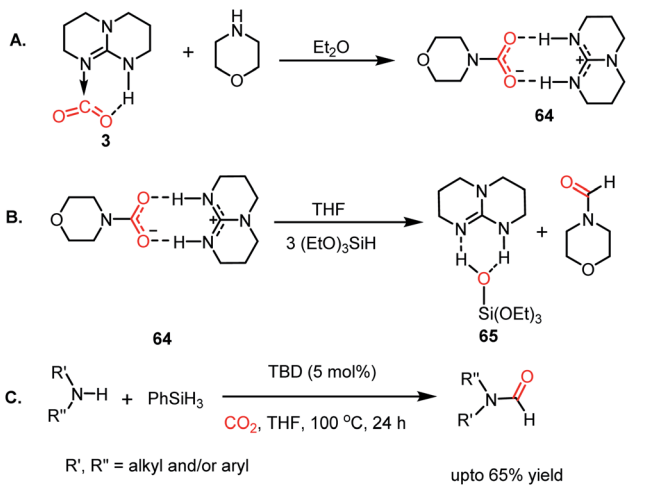

Scheme 20 (A) Formation of carbamate from TBD–CO_2 adduct and morpholine. (B) Reduction of carbamate to formamide in the presence of a silane. (C) Optimized catalytic condition for the formylation of amines using TBD as a catalyst.

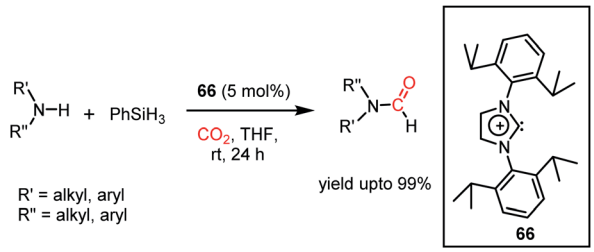

Scheme 21 Reductive functionalization of CO_2 with amines using NHC **66** as a catalyst under ambient conditions.

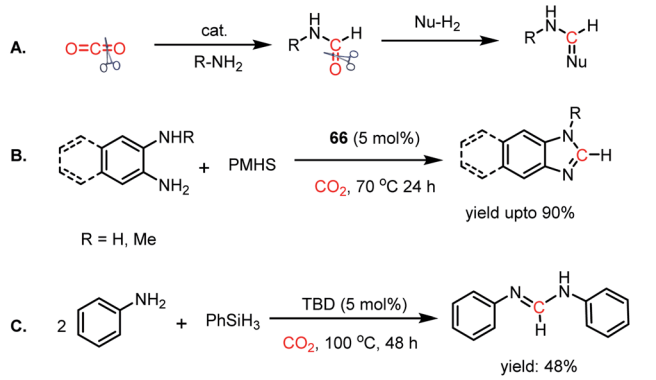

Scheme 22 (A) Deoxygenation of CO_2 *via* cascade reductive functionalization. (B) Reductive functionalization of CO_2 using diamines and IPr (**66**) as a catalyst. (C) Deoxygenation of CO_2 *via* the four-component approach.

secondary aliphatic amines, aromatic amines, imines, hydrazines, and N-heterocycles. The NHC outperformed the yield of the desired product (87%) compared to that by TBD (10%) in the case of iPr_2NH, which indicates that the steric crowding around the nitrogen centre becomes less significant due to the strong nucleophilicity of the NHC. To develop a cost effective and sustainable system, less expensive and abundant silanes were also screened, and consequently, polymethylhydrosiloxane (PMHS), which is a by-product of the silicon industry, emerged as an excellent choice, giving 90% *N*-formylmorpholine. Since PMHS is nontoxic and moisture stable, it is an ideal replacement for the expensive $PhSiH_3$. PMHS displayed good reactivity towards aliphatic and aromatic amines, hydrazines and heterocycles to form *N*-formylated products. This work represented the first metal-free system using PMHS as a reducing agent for the formylation reaction with CO_2.

Thus far, the 2e-reductive functionalization of CO_2 to form formylated products has been reported. However, the utilization of CO_2 as a building block of C1 chemicals is possible when the absolute deoxygenation of CO_2 occurs to prepare a wide array of chemicals. In 2013, Cantat and co-workers introduced a cascade reductive functionalization, which led to the complete deoxygenation of CO_2.[78] This resulted in the synthesis of various heterocycles, which have wide applications in the pharmaceutical industry. In the presence of IPr or TBD as a catalyst, CO_2 underwent reductive functionalization with *o*-diamines, and subsequent intramolecular condensation resulted in the formation of benzimidazole, quinazolinone, formamidines or their derivatives. This one pot reaction may be viewed as "cut and paste" approach, where four C–O bonds of CO_2 are chopped off to build four new bonds (C=N, C–N and C–H, Scheme 22A). However, at room temperature, this reaction was not selective towards heterocycles and a mixture of mono and diformylated products was also formed together with heterocycles.

To address this problem, an elevated temperature (70 °C) was applied to achieve selectivity. In the presence of 5 mol% IPr (**66**) and 1 atm CO_2, 1,2 diamines were efficiently transformed into benzimidazole derivatives with a yield of up to 90% using PMHS as a reducing agent at 70 °C for 24 h (Scheme 22B). Further, a 4-component reaction was accomplished, where two functionalizing agents were linked by a linker as a result of intermolecular reactions (Scheme 22C). In 2015, Kinjo *et al.* introduced a phosphorus-based catalyst for the reductive functionalization of CO_2.[79] In their work, 1,3,2-diazaphospholene (**67**) was introduced for the activation of CO_2. In the presence of CO_2 in acetonitrile-d_3 under ambient conditions, **67** underwent a rapid colour change from yellow to deep brown. The peak in the ^{31}P NMR spectrum showed a downfield shift from δ 57.8 ppm to 111.5 ppm, whereas the ^{1}H and ^{13}C NMR spectra showed new peaks at δ 8.10 ppm and 164.2 ppm, indicating the presence of a formate (**68**, Scheme 23A), which was further established by X-ray crystallography. The formation of **68** represents the first hydrophosphination of CO_2. The down-fielded ^{31}P NMR chemical shift and X-ray structure revealed that the P–O bond distance (1.808(1) Å) is 11% longer than that of the typical P–O single bond (1.63 Å), suggesting a significant contribution from the zwitterionic form (**68a**) in resonance with **68** (Scheme 23A). This ionic property of the bond that induces zwitterionic character perhaps facilitates the formate group transfer to the appropriate receptor. The

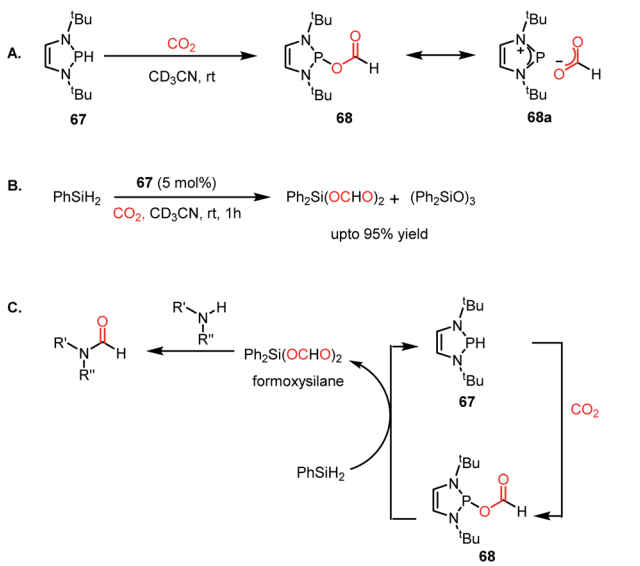

Scheme 23 (A) Activation of CO_2 by 1,3,2-diazaphospholene **67**. (B) Hydrosilylation of CO_2 in the presence of **67**. (C) Plausible mechanistic cycle for the formylation of amines using **67** as a catalyst.

reaction between **67** and a silane in a CO_2 atmosphere led to the formation of a formoxysilane (Scheme 23B). Encouraged by this result, the reductive functionalization of CO_2 in the presence of an amine was attempted. It was found that the combination of 5 mol% of **67** with diphenylsilane in the presence of acetonitrile at rt for 4 h resulted in the successful formylation of a variety of amines, which include both primary and secondary amines, with 61–99% yield. A plausible cycle was proposed, in which the first step involves the incorporation of CO_2 in the P–H bond, which in turn transfers the formate group to silane to form formoxysilane and regenerates **67**. Formoxysilane upon reaction with amines forms formamides and other by-products (Scheme 23C). This work represents the first hydrophosphination of CO_2.

In 2015, Liu and co-workers introduced ionic liquids for the formylation of amines for the first time.[80] It was found that imidazolium-based ILs could perform the *N*-formylation of various amines with CO_2 under ambient conditions using $PhSiH_3$ as a reductant. Consequently, 1-butyl-3-methylimidazolium chloride ([BMIm]Cl, **69**) emerged as an efficient catalyst for the formylation of various aromatic and aliphatic amines, resulting in up to 99% yield (Scheme 24A). The reaction between **69** and phenylsilane displayed a noticeable change in the NMR spectra, which indicates that the first step involves the activation of the Si–H bond of phenylsilane by **69**. Further, the reaction between phenylsilane and **69** in a CO_2 atmosphere led to a signal in the ^{13}C NMR spectrum at δ 163.0 ppm and δ 8.27 ppm in the ^{1}H NMR spectrum. These signals were attributed to the formation of a formoxysilane, which is the key intermediate of the reaction. This result suggests that the activation of phenylsilane by **69** favours facile insertion of CO_2. Earlier, Wang and co-workers reported this kind of silane activation for the NHC-mediated hydrosilylation of CO_2.[59] On the other hand, the reaction between **69** and *N*-methylaniline experienced a change in signal for the N–H proton of the amine. This observation may be attributed to the hydrogen bonding between the N–H proton of the amine and the anionic fragment of IL **69**.

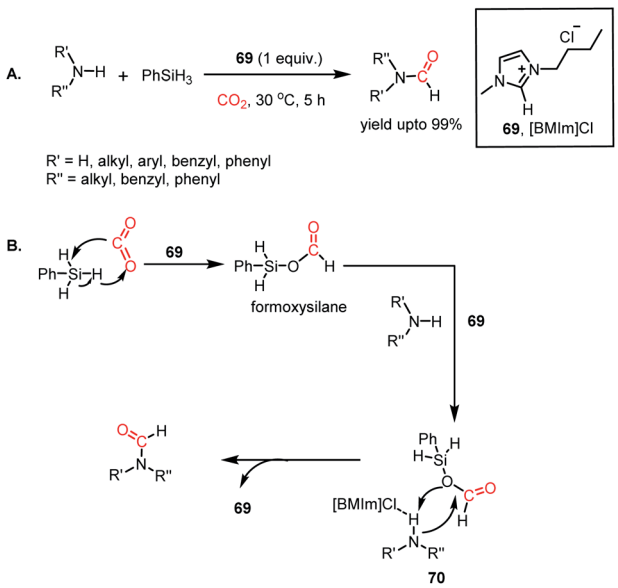

Scheme 24 (A) Ionic liquid (**69**)-mediated amine formylation with CO_2. (B) Plausible mechanistic steps for amine formylation using **69**.

Combining these observations, it can be concluded that **69** plays a dual role for the activation of phenylsilane, resulting in the insertion of CO_2 and activation of amines *via* hydrogen bonding. Based on these experimental evidence, a possible cycle was proposed, where the first step involves activation of the Si–H bond of phenylsilane by **69**, which leads to the insertion of CO_2 to form formoxysilane. Further, the N–H bond of the amine is involved in hydrogen bonding with **69**, and thus the amine nitrogen participates in a nucleophilic attack on the carbon atom of formoxysilane to yield the desired product *via* **70** (Scheme 24B). This report represents the first ionic liquid-mediated reductive functionalization of CO_2. In 2015, the same group introduced ionic liquids in cascade reductive functionalization using aminophenols for the construction of new C–S bonds to form various benzothiazole derivatives.[81] Sulphur-containing organic compounds exhibit numerous applications in the agriculture, pharmaceutical and chemical industries.[82] Benzothiazoles in particular are useful as enzyme inhibitors, anti-inflammatory agents, antioxidants and fluorescent materials. Hence there is a high demand for developing cost-effective methods for the synthesis of various benzothiazoles. Accordingly, an efficient protocol was developed using an ionic liquid, 1-butyl-3-methylimidazolium acetate ([Bmim][OAc], **71**), for the cyclization of 2-aminophenols in the presence of CO_2 and hydrosilane under ambient conditions. Using $(EtO)_3SiH$ and 0.5 MPa CO_2, different substituted 2-aminophenols and diamines were transformed into various benzothiazoles (up to yield 99%) and benzimidazoles (up to 96%) at 60 °C (Scheme 25A). The NMR spectroscopic analysis of the control reactions revealed strong hydrogen bonding interaction between **71**, 2-aminophenol and silane. A plausible mechanistic scheme was proposed, in which the first step involves activation of CO_2 by the ionic liquid to the carboxylate adduct, which further interacts with the activated silane to form formoxysilane. Subsequently, formoxysilane undergoes nucleophilic attack by the hydrogen-bonded amine to form the formylated product, which in turn takes part in intramolecular condensation to obtain the desired product (Scheme 25B). Here, IL **71** acts as a tri-functional catalyst, which activates CO_2, amine and silane to develop an efficient strategy for the synthesis of various heterocycles.

Next, the ionic liquid-mediated reductive functionalization of CO_2 resulted in the synthesis of *N*,*N*-disubstituted formamides (NNFAs). NNFA represents a class of formamides with wide applications in the pharmaceutical field, but their synthesis remains a challenging task. In 2017, Liu and co-workers further extended their ionic liquid-mediated reductive functionalization of CO_2 strategy towards the synthesis of NNFAs.[83] In their work, 1-butyl-3-methylimidazolium chloride ([BMIm]Cl, **69**)-mediated three-component coupling between CO_2, primary amines and aldehydes was developed to synthesize NNFA in the presence of phenylsilane as a reducing agent under ambient conditions. **69** was used to perform the coupling between aryl amines and aryl aldehydes followed by reductive formylation in

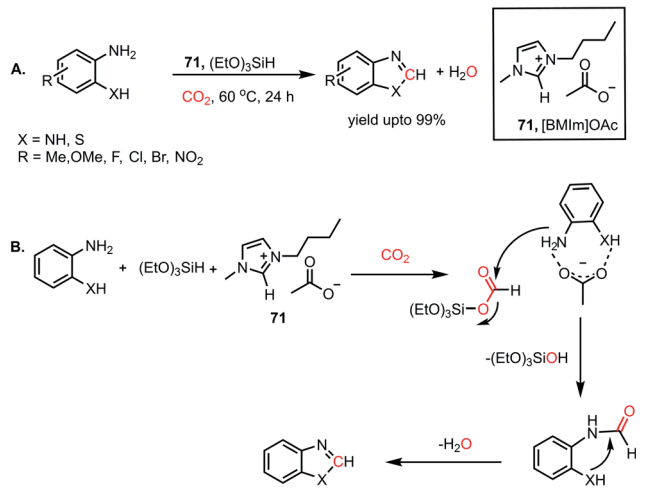

Scheme 25 (A) Ionic liquid **71**-mediated reductive functionalization of amines with CO_2 for the synthesis of heterocycles. (B) Plausible mechanistic steps for the reductive functionalization of diamines by IL **71**.

the presence of 10 atm CO_2 and $PhSiH_3$ at 30 °C to produce unsymmetrical *N*,*N* formamides in 92% yield (Scheme 26A). **69** was reused consecutively five times without loss in its activity and the process was easily scaled to gram scale. The scope of this reaction was further extended to aliphatic amines and aldehydes to synthesize various *N*,*N*-formamides with alkyl substitution. In the presence of **69**, CO_2 interacts with phenylsilane to form formoxysilane, which in turn reacts with benzylideneaniline, an *in situ* generated product by reaction between amine and aldehyde, resulting in the formation of the final product *via* **72** (Scheme 26B).

Thus far, we have seen how both the cation and anion of ILs are required simultaneously for the reductive functionalization of CO_2. In contrast, tetrabutylammonium salt as a catalyst necessitates only the involvement of its anion, whereas its cation only serves as a counterion. The steric crowding of the tetrabutylammonium cation minimizes the cation–anion interaction and allows the anion to be available in the medium to take part in reaction. In 2016, Dyson and co-workers introduced tetrabutylammonium fluoride as an efficient catalyst for the *N*-formylation of amines with CO_2 in the presence of

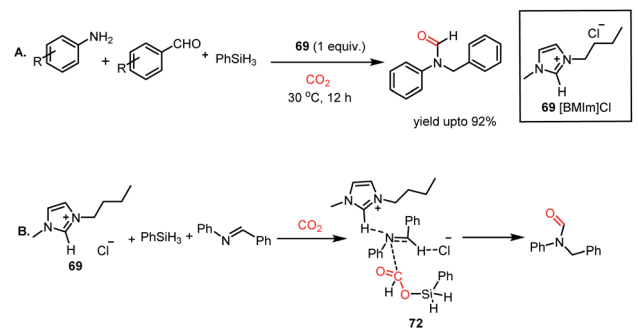

Scheme 26 (A) Ionic liquid **69**-mediated synthesis of *N*,*N*-formamides. (B) Plausible mechanistic cycle for the synthesis of NNFAs.

phenylsilane under ambient conditions.[84] It was found that in the presence of 10 mol% TBAF·$3H_2O$, various aromatic and aliphatic amines underwent formylation using phenylsilane and 0.1 MPa CO_2 at room temperature to achieve a yield of up to 94% (Scheme 27). Moreover, this was demonstrated for the synthesis of ^{11}C-labelled drug molecules using $^{11}CO_2$. In the same year, He and co-workers also reported the use of TBAF for the *N*-formylation of aromatic and aliphatic amines using triethoxysilane at 30 °C to attain a maximum yield of 99% (Scheme 27).[85]

To date, we have seen that the nucleophilicity of catalysts plays a pivotal role in activating CO_2 and its catalytic reductive functionalization. Besides nucleophilic reagents, the report by Sun and co-workers first described the electrophile-mediated catalytic reductive functionalization of CO_2.[86] $B(C_6F_5)_3$ was introduced as a catalyst for the synthesis of benzimidazoles from *o*-phenylenediamines. In the first step, the interaction of *o*-phenylenediamine with $B(C_6F_5)_3$ generates an FLP based on the amine/borane pair. In the presence of 10 mol% $B(C_6F_5)_3$ and 1 MPa of CO_2, various aryl diamines underwent formylation followed by condensation to form the corresponding benzimidazoles (Scheme 28A). A plausible mechanism was proposed, in which first $B(C_6F_5)_3$ interacts with diamine to form an N/B FLP and CO_2 interacts with the *in situ* formed FLP to form a CO_2 adduct (**74**). Secondly, $B(C_6F_5)_3$ activated $PhSiH_3$ which in turn coordinated with **74** to form intermediate **75** which lead to the release of formamide and regeneration of $B(C_6F_5)_3$. Formamide underwent subsequent condensation to release benzimidazole as the final product (Scheme 28B). In addition, several other methods were also employed for the *N*-formylation of amines using CO_2 such as thiazolium carbene,[87] N-heterocyclic olefins,[88] tetrabutylammonium-carboxylates,[89] acetates,[90] phosphorus ylides,[91] γ-valerolactone,[92] and ionic liquids.[93,94] Moreover, it was found that the catalytic formylation of amines is also possible in the presence of polar solvents such as DMF[95] and DMSO.[96] This can be attributed to the high solubility of CO_2 and the enhanced basicity of amines in polar aprotic solvents.

All the above-mentioned reports required an amine functional group to carry out the reduction. The high basicity of amines makes them suitable candidates for the reductive functionalization of CO_2. On the contrary, amides represent very weak bases and less reactive in comparison to amines because of the conjugation of their nitrogen lone pair of

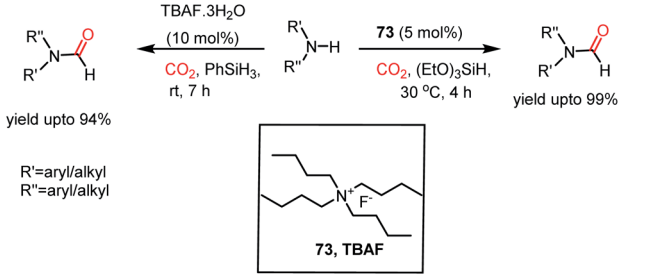

Scheme 27 Fluoride anion-mediated *N*-formylation of amines.

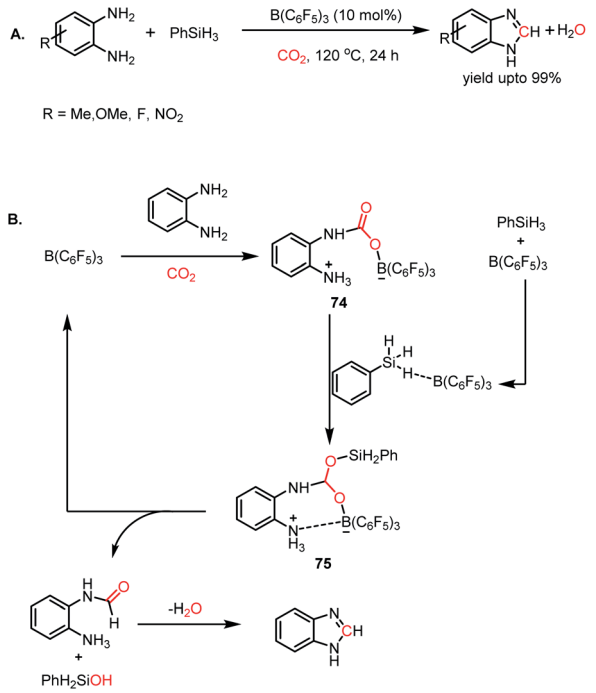

Scheme 28 (A) $B(C_6F_5)_3$-mediated catalytic *N*-formylation of *o*-diamines. (B) Plausible mechanistic cycle for the catalytic *N*-formylation of diamines.

electrons with the C=O group. In 2018, Mandal and co-workers accomplished the *N*-formylation of primary amides by CO_2 using an abnormal N-heterocyclic carbene for the first time.[97] Previously, DFT calculations showed that the HOMO of aNHC is higher in energy compared to isomeric NHC, which makes it more nucleophilic,[26] and hence can be involved in hydrogen bonding with the amide proton, facilitating its interaction with silane. It was found that 5 mol% aNHC (**48**) resulted in the reductive functionalization of primary amides with 1 atm CO_2 using phenylsilane. Various aromatic and aliphatic amides underwent facile *N*-formylation with a yield of up to 81% (Scheme 29A). Moreover, this protocol was successful in synthesizing the precursors for two natural products, alatamide and lansiumamide, which exhibit strong larvicidal activity. The reaction initiates with the formation of the aNHC–CO_2 adduct (**6**). The stoichiometric reaction between **6** and triphenylsilane in acetonitrile in the absence of CO_2 displayed a singlet at δ 8.71 ppm in ^{1}H NMR spectroscopy and a signal at δ 168.1 ppm in ^{13}C NMR spectroscopy, which confirmed the formation of a formoxysilane intermediate. Upon interaction with amide, formoxysilane transfers the formyl group to the amide molecule in the presence of another unit of silane to yield the desired product (Scheme 29B).

4.2 Aminals from CO_2

Aminals represent the 4e-reduced species of CO_2, in which carbon is reduced to C(0) from C(+4) *via* the C(+2) species. Arresting the C(0) species is a challenging task since it tends to undergo over reduction into C(−2) species. Therefore, only

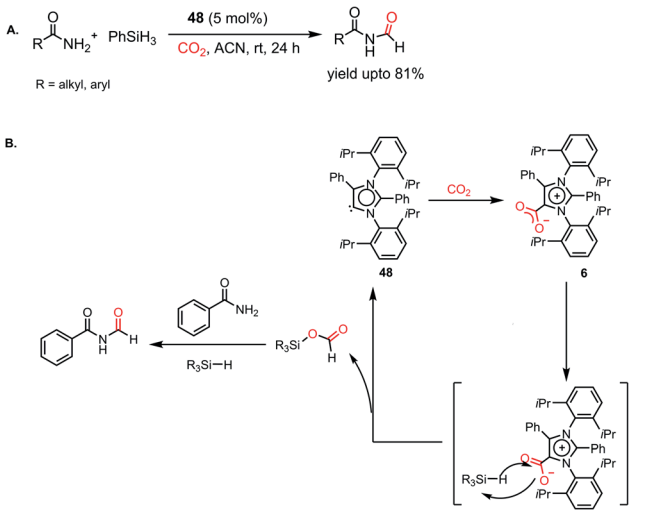

Scheme 29 (A) aNHC-mediated *N*-formylation of primary amides. (B) Plausible mechanistic cycle for the formylation of amides.

a few reports are currently available that address the metal-free reductive functionalization of CO_2 to aminals.[98,99] In 2015, Cantat and co-workers reported the first metal-free catalyst for the 4e-reductive functionalization of CO_2.[98] In the presence of 10 mol% TBD and CO_2, secondary aromatic amines underwent reduction by $PhSiH_3$ at 80 °C in acetonitrile, resulting in aminals with 98% yield (Scheme 30A).

Moreover, this strategy was extended to obtain unsymmetrical aminals using two different amines. The reaction proceeds *via* the hydrosilylation of CO_2 in the presence of TBD to form silyl acetals. The silyl acetal further undergoes sequential nucleophilic attack by amines to form the desired product (Scheme 30B).

4.3 Catalytic *N*-methylation by CO_2

The use of CO_2 as a reagent for methylation represents a 6e-reduction process. CO_2 can undergo reductive

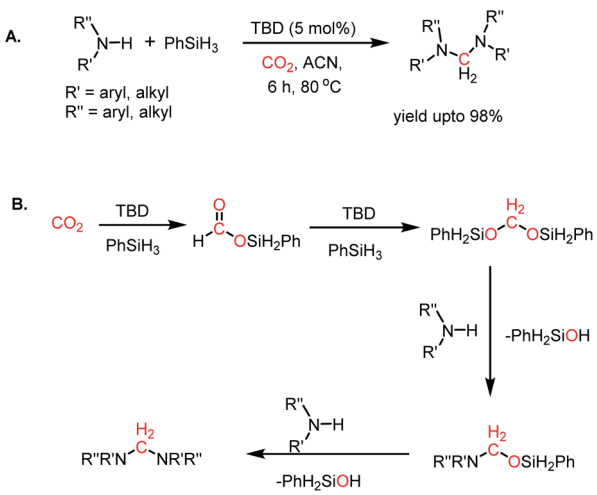

Scheme 30 (A) Catalytic reductive functionalization of CO_2 with amines to form aminals using TBD. (B) Mechanistic steps for aminal formation.

functionalization with amines to formylamines, which upon further reduction, leads to methylamines. Earlier, the *N*-methylation of amines by CO_2 used various transition metal catalysts such as Ru, Cu, and Zn.[100–102] In addition to the use of expensive metals, these systems required harsh reaction conditions, such as high pressure and temperature. In 2014, Cantat and co-workers introduced the first metal-free catalytic methylation of amines using CO_2, in which a phosphine was used as the catalyst (Scheme 31A).[103] The affinity of phosphine toward borane to form a phosphine–borane adduct facilitates the hydride transfer process, and hence hydroboranes were chosen as the reductants for this transformation. Proazaphosphatrane (**76**) is known to have superior basicity over classical phosphines owing to the pπ–dπ back bonding from the lone pairs of electrons from nitrogen centres. **76** catalysed the *N*-methylation of aromatic and aliphatic secondary amines in the presence of CO_2 and 9-BBN at 90 °C with yield up to 99%. Furthermore, in the presence of excess borane, primary amines also underwent *N*-methylation. This study was further extended to the one-pot reduction and reductive functionalization, in which the nitro group undergoes reduction to form an amine *in situ*, which is further reduced to methylamine in the presence of CO_2. It was found that amines undergo reduction by 9-BBN to afford *N*-borylated amine *via* the elimination of H_2 (Scheme 31B). Simultaneously, the formoxyborane formed by the reduction of CO_2 in the presence of 9-BBN and the catalyst interacts with *N*-borylated amine to form *N*-formyl-amine, forming a new C–N bond. *N*-Formyl-amine undergoes further reduction to yield the methylamine. The elevated temperature favours the reaction to undergo reductive functionalization over reduction.

In the same year, Dyson and co-workers introduced N-heterocyclic carbenes as metal-free catalysts for the *N*-methylation of amines using CO_2.[104] It was found that IMes (77) could perform the *N*-methylation of various aromatic, heteroaromatic, and aliphatic amines with CO_2 in the presence of Ph_2SiH_2 as a reducing agent at 50 °C with a yield of up to 91% (Scheme 32). This catalytic protocol was efficient in preparing an antifungal agent naftifine **78** with an overall yield of 58% (Scheme 32). Moreover, this method exhibited good functional group

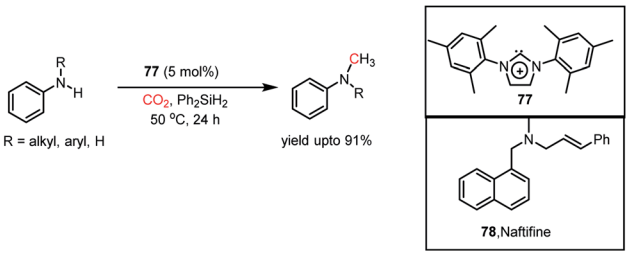

Scheme 32 Catalytic methylation of amines by CO_2 using **77**.

tolerance, in which NO_2, CN, ester, double and triple bonds were well-tolerated.

Instead of bivalent carbene possessing a pair of electrons, it was thought carbodicarbene (CDC), having an additional pair of electrons on the C(0) centre, may have enhanced nucleophilicity for the activation of CO_2. In 2008, the first CDC molecules were synthesized,[105,106] and subsequently, these CDC molecules were successfully introduced with suitable metal ions in catalysis for various organic transformations.[107] In 2015, Ong and co-workers developed a series of unsymmetrical carbodicarbenes.[108] These CDCs were utilized as metal-free catalysts in the *N*-methylation of amines using CO_2 in the presence of 9-BBN (Scheme 33A). In the presence of 10 mol% CDC **79** and 9-BBN, primary and secondary amines underwent *N*-methylation using CO_2 in toluene at 100 °C to give a yield of up to 90%. The stoichiometric reaction between **79** and 9-BBN resulted in the formation of the CDC–BBN adduct **80**, which was characterised *via* X-ray crystallography. It was found that the hydrogen of 9-BBN migrated to the carbodicarbene, which was also confirmed by the signal at δ 5.26 ppm in the ^{1}H NMR spectrum. The catalytic reaction performed using **80** also yielded the desired product in 90% yield, which indicates that **80** is a catalytic intermediate. In the presence of CO_2, the 9-BBN unit present in

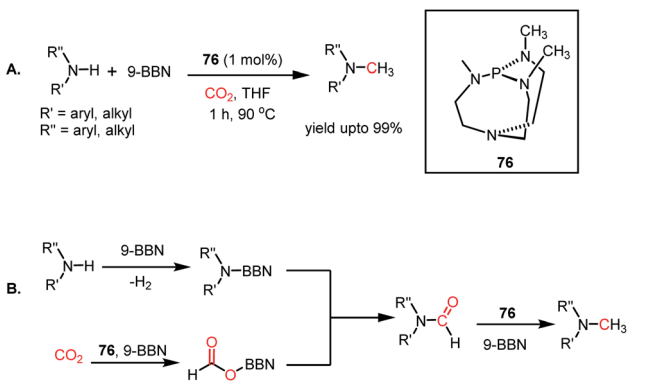

Scheme 31 (A) Methylation of amines by proazaphosphatrane **76** in the presence of CO_2. (B) Plausible mechanistic steps for the catalytic methylation of amines by **76** using CO_2.

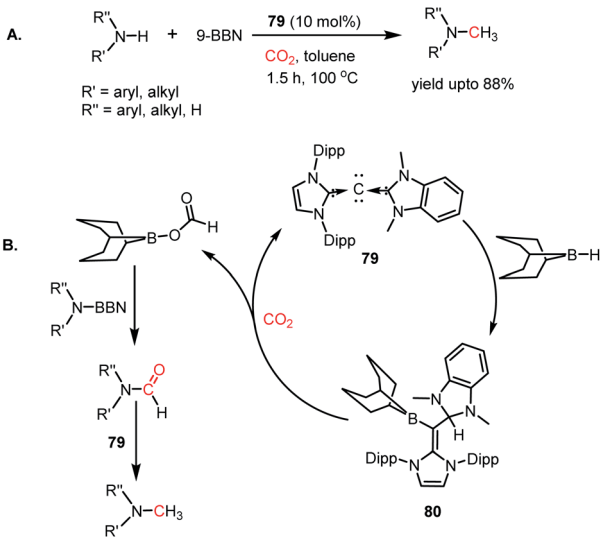

Scheme 33 (A) Methylation of amines using CO_2 in the presence of carbodicarbene **79**. (B) Plausible mechanistic cycle for the methylation of amines.

80 migrates to CO_2 to form boronformate, which reacts with *N*-borylated amine formed *in situ* to produce *N*-formylated amines. In the presence of **79**, the *N*-formylated amine undergoes further reduction to yield *N*-methylated amines (Scheme 33B).

In addition to nucleophiles, electrophiles were also used for the methylation of amines. In 2015, Liu and co-workers introduced $B(C_6F_5)_3$ for the reductive functionalization of CO_2 to form methylamines.[109] 5 mol% $B(C_6F_5)_3$ in the presence of phenylsilane resulted in the *N*-methylation of primary and secondary amines in 93% yield using a CO_2 pressure of 0.5 MPa (Scheme 34A). The reaction proceeds *via* a synergistic pathway, in which $B(C_6F_5)_3$ plays a triple role in activating all the reagents. $B(C_6F_5)_3$ activates phenylsilane *via* a non-covalent interaction between the hydride and B centre (Scheme 34B). On the other hand, the presence of polar C–F bonds in $B(C_6F_5)_3$ makes it suitable for electrostatic interaction with the carbon centre of CO_2, leading to its activation. Simultaneously, amine can interact with $B(C_6F_5)_3$ owning to the strong electrostatic interaction between nitrogen and boron, which was evident from NMR spectroscopy. These synergistic activations led to the formylation of amine, which in turn underwent reduction to generate methylamines. In addition to these reports, the catalytic methylation of amines was also carried out using DBU.[110] Lei and co-workers reported that an aprotic polar solvent such as DMF can also promote the *N*-methylation reaction.[111]

The previous section described how different metal-free catalysts were used to enable the reductive functionalized products. However, none of the them could perform the hierarchical reduction of CO_2, in which a single catalyst can control the kinetics to obtain a range of reduced products sequentially. In this regard, in 2017, He and co-workers introduced glycine betaine (GB) **81** as a metal-free catalyst, which represents a zwitterionic salt consisting of tetraammonium cation and carboxylate anion.[112] By regulating the CO_2 pressure, **81** successfully produced formamides or aminals or methylamine. It was found that in the presence of 10 bar of CO_2 at 50 °C, amines underwent *N*-formylation, whereas 1 bar CO_2 at 70 °C gave methylamines. Aminals were formed when CO_2 was restricted to one equiv. with respect to amine in a closed system at 50 °C (Scheme 35A). It was proposed that the first step involves the nucleophilic attack by the oxygen centre of the catalyst to the silicon centre of hydrosilane to form a hypervalent silicon species (**82**) (Scheme 35B). Next, the active hydride inserts a molecule of CO_2 to form a silylformate, regenerating

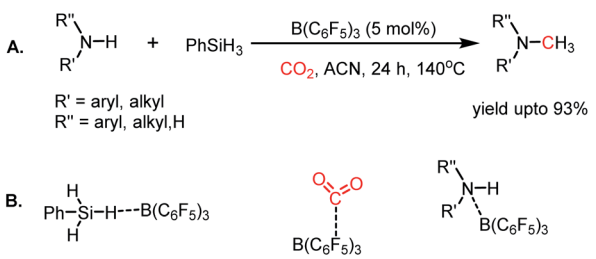

Scheme 34 (A) Methylation of amines by CO_2 in the presence of $B(C_6F_5)_3$. (B) Triple role of $B(C_6F_5)_3$ for the activation of all the reagents.

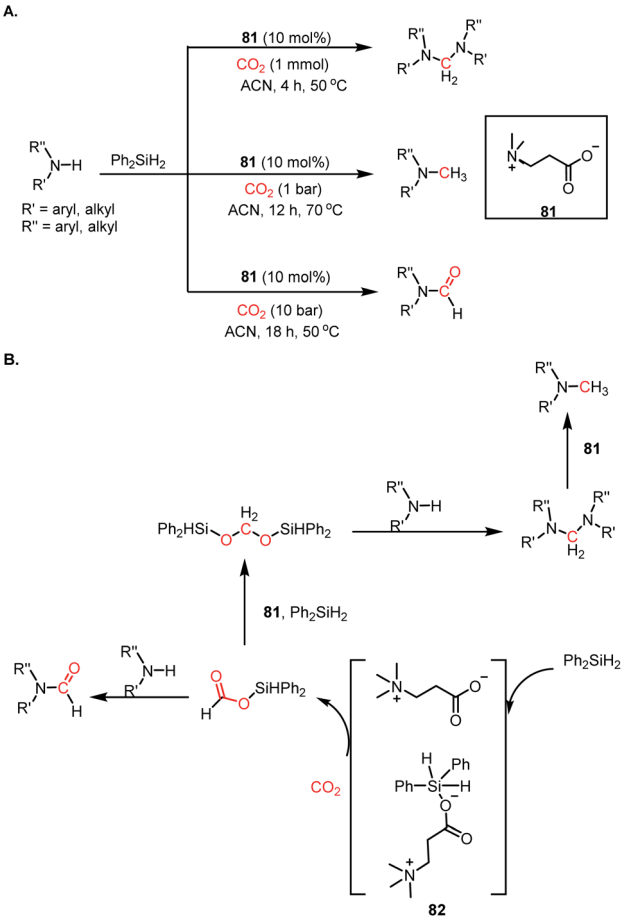

Scheme 35 (A) Hierarchical reductive functionalization of CO_2 with amines using **81**. (B) Plausible mechanistic cycle of the hierarchical reductive functionalization of CO_2.

the catalyst. At a high pressure of CO_2 (10 bar), amines interact with silylformates to form the formylated product. The excess pressure of CO_2 enhances the rate of formation of silylformate, consuming all the silanes, and hence no further reduction is possible. In the presence of excess silane, silylformate undergoes further reduction to form silylacetal, which in the presence of amine is transformed to aminals *via* condensation. Aminals may be transformed into methylamines in the presence of additional silane and catalyst (Scheme 35B). Subsequently, Nguyen *et al.* also reported the hierarchical reductive functionalization of CO_2 with amines using *N*,*N*,*N*′,*N*′-tetramethylguanidine (TMG) as the catalyst with less control over the selectivity.[113]

5. Future outlook and conclusions

During the last decade, we have witnessed the emergence of metal-free catalysts as efficient alternatives to transition metal-based catalysts for CO_2 reduction. The stoichiometric activation of CO_2 to catalytic reduction has come a long way, and thus, herein, we attempted to showcase this journey. Specifically, there are a few methods available for the catalytic reduction of

CO_2 into various chemicals and fuels on the laboratory scale under completely metal-free conditions. Moreover, these reductive transformations take place under very mild conditions. This is attributed to the combination of metal-free catalysts with silane or borane having optimal reduction potential to reduce the C–O bond. However, to translate these successes from the bench to market, one must pay serious attention to a number of factors. The marketability of these reduction processes will ultimately depend on their competitiveness between the market values of these products set by the petrochemical industry, which can be only addressed by making the process sustainable. Obviously, the catalytic reduction of thermodynamically inert C1 feedstock such as CO_2 for the production of fuels and chemicals is a significant challenge in catalysis for several reasons.

Firstly, the choice of the hydride donor or the reductant is very important, which is largely driven by its commercial availability, cost, and reactivity together with its selectivity and ease of handling. In this regard, Cantat in his excellent review discussed various hydride donors and their advantages/disadvantages in reduction chemistry.[114] Accordingly, dihydrogen, which is cheap and obtained through fossil technology, has been extensively utilized on the industrial scale, but its use for CO_2 reduction generally requires harsh reaction conditions and transition metal-based catalysts, making this process economically less attractive. Thermodynamically, the reduction of CO_2 producing C–H bonds requires only low energy since the redox potential of CO_2 couples falls within the range of 0.17 to −0.47 V *vs.* NHE (25 °C; pH = 0).[114] Thus, the reduction of CO_2 does not require a strong reductant such as the commercially available $LiAlH_4$ having quite a negative redox potential of E^0 (Al^{3+}, H_2/AlH_4^-) = −1.78 V (*vs.* NHE).[115] This negative redox potential leads to a large overpotential, and thus a high energy cost. Consequently, the use of common reducing agents such as $LiAlH_4$ and $NaBH_4$ in the large-scale reduction of CO_2 is not very attractive. In addition, their use is not atom-economic, which leads to the formation of a stoichiometric amount of waste.

On the other hand, hydrosilane or hydroborane as a reductant is very attractive from both thermodynamic and kinetic viewpoints. Their redox potential falls just in the optimum range (−0.6 V to 0 V ($E^0(B(OMe)_3/HB(OMe)_2)$ = −0.54 V and $E^0((Me_3Si)_2O/Me_3SiH)$ = −0.1 V *vs.* NHE),[114] and matches very well with the required energy input for C–O bond reduction. Moreover, they are commercially available. Especially, polymethylhydrosiloxane (PMHS), which is a byproduct of the silicon industry, and tetramethyldisiloxane (TMDS) are cheap and non-toxic with great ease in handling since they are stable in moisture and air. The optimal reduction potential of these reductants brings significant advantages in achieving enhanced chemoselectivity. However, the major pitfall of the hydrosilylation/hydroboration method arises from the formation of strong Si–O and B–O bonds, driving the reactions towards the forward direction. The formation of oxidized products such as siloxanes or boroxanes is the major drawback, making the process non-atom economic. The currently available recycling process of these siloxanes or boroxanes to hydrosilanes or hydroboranes is chemically highly energy intensive. Consequently, hydrosilanes and hydroboranes are considered as disposable hydrides. In this regard, an electrochemical approach over the chemical route may be attractive, leading to the electro-organo-recycling of these hydrides. The utilization of silanes or boranes in CO_2 reduction chemistry will remain in its infancy unless cost-efficient methods are developed to regenerate them (Scheme 36).

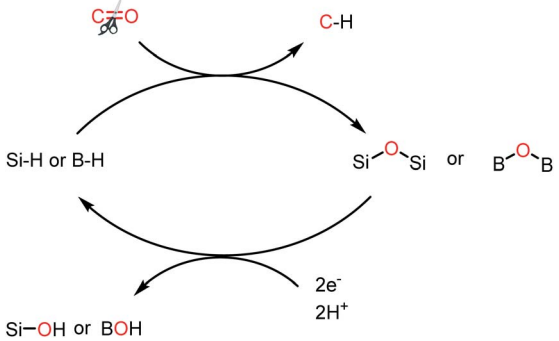

Scheme 36 Use of silane and borane for the reduction of CO_2 will be sustainable if they can be recycled in an energy efficient way.

Additionally, for translating the metal-free catalytic CO_2 reduction into an industrial process, one must heterogenize the process by immobilizing the catalyst on a solid support. The heterogenization of the metal-free catalyst will make the process sustainable in terms of recyclability. In this regard, a few heterogenous catalysts have been developed thus far. In 2016, Zhang and co-workers reported a solid poly-N-heterocyclic carbene for the reductive functionalization of CO_2 in the presence of amine.[116] Later, two more reports emerged using porous organic polymers[117] and nitrogen-doped graphene nanosheets.[118] These initial reports on heterogeneous processes using metal-free catalysts are certainly encouraging towards translating this laboratory process to a scaled-up process.

Finally, as a note of caution, one must pay attention to the environmental sustainability by considering the life cycle assessment (LCA)[119,120] of the CCR process. The practical potential of this process relies on its overall energy efficiency, including both the capture of CO_2 and its utilization, which require energy. The supply of energy may lead to indirect CO_2 emission. Thus, the anticipated environmental advantages of CCR may not be guaranteed always, for example, a tediously accomplished CCR process may finally be environmentally less sustainable than a classical fossil-based route. Thus, whether or not a specific CCR process is favorable from the viewpoint of environmental sustainability, one must consider its life cycle assessment (LCA), which takes into account the entire life cycle of products and processes, from the extraction of raw materials to the final disposal of waste, with respect to environmental impacts such as fossil resource depletion, global warming, and toxicities.

Moreover, as mentioned in the beginning, only a limited extent of total CO_2 emissions are currently utilized in chemical conversion to value-added products, although this can be potentially expanded. To achieve this goal, one must improve

the scope of chemicals available from the reduction of CO_2, which presently remains very narrow in comparison to that currently available from fossil technology. For example, the basic functional groups encountered frequently in organic chemistry, such as ketones, amides and esters, featuring a carbon atom that is reduced, are unavailable from carbon dioxide currently. Thus, this chemical reduction is certainly welcome in the future to broaden the horizon of CO_2 reduction chemistry. To translate these initial successes into practical applications, multidisciplinary approaches combining metal-free catalysts immobilized on a suitable support together with the recycling of hydrosilanes or hydroboranes through electrochemical methods can offer an appealing strategy in the catalytic reduction chemistry of CO_2.

Conflicts of interest

The authors declare no competing financial interest.

Acknowledgements

We thank the STARS Program (Grant No. STARS/APR2019/CS/473/FS) of India. SP thanks DST-Inspire for research fellowship.

References

1 (*a*) IEA, *Annual change in global energy-related CO_2 emissions, 1900-2020*, IEA, Paris, https://www.iea.org/data-and-statistics/charts/annual-change-in-global-energy-related-CO2-emissions-1900-2020; (*b*) https://www.iea.org/articles/the-impact-of-the-covid-19-crisis-on-clean-energy-progress; (*c*) *Global CO_2 emissions in 2019*, IEA, Paris, https://www.iea.org/articles/global-CO2-emissions-in-2019.
2 C. Figueres, C. Le Quéré, A. Mahindra, O. Bäte, G. Whiteman, G. Peters and D. Guan, *Nature*, 2018, **564**, 27–30, Intergovernmental Panel on Climate Change. Global Warming of 1.5 °C (IPCC, 2018).
3 (*a*) D. Y. C. Leung, G. Caramanna and M. M. Maroto-Valer, *Renewable Sustainable Energy Rev.*, 2014, **39**, 426–443; (*b*) H. De Coninck and S. M. Benson, *Annual Review of Environment and Resources*, 2014, 243–270; (*c*) T. Bruhn, H. Naims and B. Olfe-Kräutlein, *Environ. Sci. Policy*, 2016, **60**, 38–43.
4 E. A. Quadrelli, G. Centi, J.-L. Duplan and S. Perathoner, *ChemSusChem*, 2011, **4**, 1194–1215.
5 J. Klankermayer, S. Wesselbaum, K. Beydoun and W. Leitner, *Angew. Chem., Int. Ed.*, 2016, **55**, 7296–7343.
6 A. Tlili, E. Blondiaux, X. Frogneux and T. Cantat, *Green Chem.*, 2015, **17**, 157–168.
7 C. Federsel, A. Boddien, R. Jackstell, R. Jennerjahn, P. J. Dyson, R. Scopelliti, G. Laurenczy and M. Beller, *Angew. Chem., Int. Ed.*, 2010, **49**, 9777–9780.
8 C. A. Huff and M. S. Sanford, *J. Am. Chem. Soc.*, 2011, **133**, 18122–18125.
9 S. Bontemps, L. Vendier and S. Sabo-Etienne, *Angew. Chem., Int. Ed.*, 2012, **51**, 1671–1674.
10 S. Bontemps, L. Vendier and S. Sabo-Etienne, *J. Am. Chem. Soc.*, 2014, **136**, 4419–4425.
11 G. Fiorani, W. Guo and A. W. Kleij, *Green Chem.*, 2015, **17**, 1375–1389.
12 F.-G. Fontaine, M.-A. Courtemanche and M.-A. Légaŕe, *Chem.–Eur. J.*, 2014, **20**, 2990–2996.
13 F.-G. Fontaine and D. W. Stephan, *Current Opinion in Green and Sustainable Chemistry*, 2017, **3**, 28–32.
14 X.-F. Liu, X. Y. Li, C. Qiao and L.-N. He, *Synlett*, 2018, **29**, 548–555.
15 H. Zhou and X. Lu, *Sci. China: Chem.*, 2017, **60**, 904–911.
16 M. Hulla and P. J. Dyson, *Angew. Chem., Int. Ed.*, 2020, **59**, 1002–1017.
17 Y. Zhang, T. Zhang and S. Das, *Green Chem.*, 2020, **22**, 1800–1820.
18 C. C. Chong and R. Kinjo, *ACS Catal.*, 2015, **5**, 3238–3259.
19 F. J. Fernández-Alvarez, A. M. Aitani and L. A. Oro, *Catal. Sci. Technol.*, 2014, **4**, 611–624.
20 A. Álvarez, A. Bansode, A. Urakawa, A. V. Bavykina, T. A. Wezendonk, M. Makkee, J. Gascon and F. Kapteijn, *Chem. Rev.*, 2017, **117**, 9804–9838.
21 J. Schneider, H. Jia, J. T. Muckerman and E. Fujita, *Chem. Soc. Rev.*, 2012, **41**, 2036–2051.
22 D. H. Gibson, *Coord. Chem. Rev.*, 1999, **185–186**, 335–355.
23 J. R. Ellis, *Nature*, 2010, **463**, 164–165.
24 M. Iwatani, K. Kudo, N. Sugita and Y. Takezaki, *Sekiyu Gakkaishi*, 1978, **21**, 290–296.
25 E. R. Pérez, M. O. da Silva, V. C. Costa, U. P. Rodrigues-Filho and D. W. Franco, *Tetrahedron Lett.*, 2002, **43**, 4091–4093.
26 E. R. Pérez, R. H. A. Santos, M. T. P. Gambardella, L. G. M. d. Macedo, U. P. Rodrigues-Filho, J.-C. Launay and D. W. Franco, *J. Org. Chem.*, 2004, **69**, 8005–8011.
27 C. Villiers, J.-P. Dognon, R. Pollet, P. Thuéry and M. Ephritikhine, *Angew. Chem., Int. Ed.*, 2010, **49**, 3465–3468.
28 A. J. Arduengo, R. L. Harlow and M. J. Kline, *J. Am. Chem. Soc.*, 1991, **113**, 361–363.
29 (*a*) N. Kuhn, E. Niquet, M. Steimann and I. Walker, *Z. Naturforsch., B: Anorg. Chem., Org. Chem.*, 1999, **54**, 427–433; (*b*) H. A. Duong, T. N. Tekavec, A. M. Arif and J. Louie, *Chem. Commun.*, 2004, 112–113.
30 E. Aldeco-Perez, A. J. Rosenthal, B. Donnadieu, P. Parameswaran, G. Frenking and G. Bertrand, *Science*, 2009, **326**, 556–559.
31 G. Kuchenbeiser, M. Soleilhavoup, B. Donnadieu and G. Bertrand, *Chem.–Asian J.*, 2009, **4**, 1745–1750.
32 E. D. Bates, R. D. Mayton, I. Ntai and J. H. Davis, *J. Am. Chem. Soc.*, 2002, **124**, 926–927.
33 C. M. Wang, H. M. Luo, D. E. Jiang, H. R. Li and S. Dai, *Angew. Chem., Int. Ed.*, 2010, **49**, 5978–5981.
34 H. C. Brown, H. I. Schlesinger and S. Z. Cardon, *J. Am. Chem. Soc.*, 1942, **64**, 325–329.
35 G. Wittig and E. Benz, *Chem. Ber.*, 1959, **92**, 1999–2013.
36 W. Tochtermann, *Angew. Chem., Int. Ed. Engl.*, 1966, **5**, 351–371.
37 D. J. Parks and W. E. Piers, *J. Am. Chem. Soc.*, 1996, **118**, 9440–9441.

38 S. Rendler and M. Oestreich, *Angew. Chem., Int. Ed.*, 2008, **47**, 5997–6000.
39 G. C. Welch, R. R. San Juan, J. D. Masuda and D. W. Stephan, *Science*, 2006, **314**, 1124–1126.
40 C. M. Mömming, E. Otten, G. Kehr, R. Fröhlich, S. Grimme, D. W. Stephan and G. Erker, *Angew. Chem., Int. Ed.*, 2009, **48**, 6643–6646.
41 P. G. Jessop, F. Jo and C.-C. Tai, *Coord. Chem. Rev.*, 2004, **248**, 2425–2442.
42 G. A. Olah, *Angew. Chem., Int. Ed.*, 2005, **44**, 2636–2639.
43 D. H. Gibson, *Chem. Rev.*, 1996, **96**, 2063–2096.
44 A. E. Ashley, A. L. Thompson and D. O'Hare, *Angew. Chem., Int. Ed.*, 2009, **48**, 9839–9843.
45 V. Sumerin, F. Schulz, M. Nieger, M. Leskela, T. Repo and B. Rieger, *Angew. Chem., Int. Ed.*, 2008, **47**, 6001–6003.
46 A. Berkefeld, W. E. Piers and M. Parvez, *J. Am. Chem. Soc.*, 2010, **132**, 10660–10661.
47 A. Berkefeld, W. E. Piers, M. Parvez, L. Castro, L. Maron and O. Eisenstein, *Chem. Sci.*, 2013, **4**, 2152–2162.
48 M.-A. Courtemanche, M.-A. Légaŕe, L. Maron and F.-G. Fontaine, *J. Am. Chem. Soc.*, 2013, **135**, 9326–9329.
49 M.-A. Courtemanche, M.-A. Légaŕe, L. Maron and F.-G. Fontaine, *J. Am. Chem. Soc.*, 2014, **136**, 10708–10717.
50 R. Declercq, G. Bouhadir, D. Bourissou, M.-A. Légaré, M.-A. Courtemanche, K. S. Nahi, N. Bouchard, F.-G. Fontaine and L. Maron, *ACS Catal.*, 2015, **5**, 2513–2520.
51 T. Wang and D. W. Stephan, *Chem. Commun.*, 2014, **50**, 7007–7010.
52 J. M. Farrell, J. A. Hatnean and D. W. Stephan, *J. Am. Chem. Soc.*, 2012, **134**, 15728–15731.
53 T. Wang and D. W. Stephan, *Chem.–Eur. J.*, 2014, **20**, 3036–3039.
54 N. von Wolff, G. Lefevre, J.-C. Berthet, P. Thuéry and T. Cantat, *ACS Catal.*, 2016, **6**, 4526–4535.
55 A. Ramos, A. Antiñolo, F. Carrillo-Hermosilla, R. Fernández-Galán, A. Rodríguez-Diéguez and D. García-Vivó, *Chem. Commun.*, 2018, **54**, 4700–4703.
56 R. Boese, R. Köster and M. Yalpani, *Z. Naturforsch., B: J. Chem. Sci.*, 1994, **49**, 1453–1458.
57 M. A. Courtemanche, A. P. Pulis, É. Rochette, M. A. Légaré, D. W. Stephan and F. G. Fontaine, *Chem. Commun.*, 2015, **51**, 9797–9800.
58 S. N. Riduan, Y. Zhang and J. Y. Ying, *Angew. Chem., Int. Ed.*, 2009, **48**, 3322–3325.
59 F. Huang, G. Lu, L. Zhao, H. Li and Z.-X. Wang, *J. Am. Chem. Soc.*, 2010, **132**, 12388–12396.
60 S. N. Riduan, J. Y. Ying and Y. Zhang, *ChemCatChem*, 2013, **5**, 1490–1496.
61 S. C. Sau, R. Bhattacharjee, P. K. Vardhanapu, G. Vijaykumar, A. Datta and S. K. Mandal, *Angew. Chem., Int. Ed.*, 2016, **55**, 15147–15151.
62 S. C. Sau, R. Bhattacharjee, P. K. Hota, P. K. Vardhanapu, G. Vijaykumar, R. Govindarajan, A. Datta and S. K. Mandal, *Chem. Sci.*, 2019, **10**, 1879–1884.
63 C. Das Neves Gomes, E. Blondiaux, P. Thuéry and T. Cantat, *Chem.–Eur. J.*, 2014, **23**, 7098–7106.
64 Y. Yang, M. Xu and D. Song, *Chem. Commun.*, 2015, **51**, 11293–11296.
65 Y. Yang, L. Yan, Q. Xie, Q. Liang and D. Song, *Org. Biomol. Chem.*, 2017, **15**, 2240–2245.
66 D. Mukherjee, D. F. Sauer, A. Zanardi and J. Okuda, *Chem.–Eur. J.*, 2016, **22**, 7730–7733.
67 Z. Lu, H. Hausmann, S. Becker and H. A. Wegner, *J. Am. Chem. Soc.*, 2015, **137**, 5332–5335.
68 C.-H. Lim, S. Ilic, A. Alherz, B. T. Worrell, S. S. Bacon, J. T. Hynes, K. D. Glusac and C. B. Musgrave, *J. Am. Chem. Soc.*, 2019, **141**, 272–280.
69 M.-A. Courtemanche, M.-A. Légaré, E. Rochette and F.-G. Fontaine, *Chem. Commun.*, 2015, **51**, 6858–6861.
70 K. Fujiwara, S. Yasuda and T. Mizuta, *Organometallics*, 2014, **33**, 6692–6695.
71 S. Y.-F. Ho, C.-W. So, N. Saffon-Merceron and N. Mézailles, *Chem. Commun.*, 2015, **51**, 2107–2110.
72 W. Huang, T. Roisnel, V. Dorcet, C. Orione and E. Kirillov, *Organometallics*, 2020, **39**, 698–710.
73 C. Das Neves Gomes, O. Jacquet, C. Villiers, P. Thuéry, M. Ephritikhine and T. Cantat, *Angew. Chem., Int. Ed.*, 2012, **51**, 187–190.
74 S. Schreiner, J. Y. Yu and L. Vaska, *J. Chem. Soc., Chem. Commun.*, 1988, 602–603.
75 C. J. Gerack and L. McElwee-White, *Molecules*, 2014, **19**, 7689–7713.
76 R. Walsh, *Acc. Chem. Res.*, 1981, **14**, 246–252.
77 O. Jacquet, C. Das Neves Gomes, M. Ephritikhine and T. Cantat, *J. Am. Chem. Soc.*, 2012, **134**, 2934–2937.
78 O. Jacquet, C. D. N. Gomes, M. Ephritikhine and T. Cantat, *ChemCatChem*, 2013, **5**, 117–120.
79 C. C. Chong and R. Kinjo, *Angew. Chem., Int. Ed.*, 2015, **54**, 12116–12120.
80 L.-D. Hao, Y.-F. Zhao, B. Yu, Z.-Z. Yang, H.-Y. Zhang, B.-X. Han, X. Gao and Z.-M. Liu, *ACS Catal.*, 2015, **5**, 4989–4993.
81 X. Gao, B. Yu, Z.-Z. Yang, Y.-F. Zhao, H.-Y. Zhang, L.-D. Hao, B.-X. Han and Z.-M. Liu, *ACS Catal.*, 2015, **5**, 6648–6652.
82 Y. Xi, B. Dong, E. J. McClain, Q. Wang, T. L. Gregg, N. G. Akhmedov, J. L. Peterson and X. Shi, *Angew. Chem., Int. Ed.*, 2014, **53**, 4657–4661.
83 Z.-G. Ke, L.-D. Hao, X. Gao, H.-Y. Zhang, Y.-F. Zhao, B. Yu, Z.-Z. Yang, Y. Chen and Z.-M. Liu, *Chem.–Eur. J.*, 2017, **23**, 9721–9725.
84 M. Hulla, F. D. Bobbink, S. Das and P. J. Dyson, *ChemCatChem*, 2016, **8**, 3338–3342.
85 X.-F. Liu, R. Ma, C. Qiao, H. Cao and L.-N. He, *Chem.–Eur. J.*, 2016, **22**, 16489–16493.
86 Z. Zhang, Q. Sun, C. Xia and W. Sun, *Org. Lett.*, 2016, **18**, 6316–6319.
87 S. Das, F. D. Bobbink, S. Bulut, M. Soudan and P. J. Dyson, *Chem. Commun.*, 2016, **52**, 2497–2500.
88 V. B. Saptal and B. M. Bhanage, *ChemSusChem*, 2016, **9**, 1980–1985.
89 X. F. Liu, C. Qiao, X. Y. Li and L. N. He, *Green Chem.*, 2017, **19**, 1726–1731.

90 T. Murata, M. Hiyoshi, M. Ratanasak, J.-ya. Hasegawa and T. Ema, *Chem. Commun.*, 2020, **56**, 5783–5786.
91 H. Zhou, G. X. Wang, W. Z. Zhang and X. B. Lu, *ACS Catal.*, 2015, **5**, 6773–6779.
92 J. Song, B. Zhou, H. Liu, C. Xie, Q. Meng, Z. Zhang and B. X. Han, *Green Chem.*, 2016, **18**, 3956–3961.
93 X.-Y. Li, H.-C. Fu, X.-F. Liu, S.-H. Yang, K.-H. Chen and L.-N. He, *Catal. Today*, DOI: 10.1016/j.cattod.2020.01.030.
94 W. F. Zhao, X. P. Chi, H. Li, J. He and S. Yang, *Green Chem.*, 2019, **21**, 567–577.
95 T.-X. Zhao, G.-W. Zhai, J. Liang, P. Li, X.-B. Hu and Y.-T. Wu, *Chem. Commun.*, 2017, **53**, 8046–8049.
96 H. Lv, Q. Xing, C. Yue, Z. Lei and F. Li, *Chem. Commun.*, 2016, **52**, 6545–6548.
97 P. K. Hota, S. C. Sau and S. K. Mandal, *ACS Catal.*, 2018, **8**, 11999–12003.
98 X. Frogneux, E. Blondiaux, P. Thuery and T. Cantat, *ACS Catal.*, 2015, **5**, 3983–3987.
99 X.-Y. Li, S.-S. Zheng, X.-F. Liu, Z.-W. Yang, T.-Y. Tan, A. Yu and L.-N. He, *ACS Sustainable Chem. Eng.*, 2018, **6**, 8130–8135.
100 O. Jacquet, X. Frogneux, C. Das Neves Gomes and T. Cantat, *Chem. Sci.*, 2013, **4**, 2127–2131.
101 Y. Li, X. Fang, K. Junge and M. Beller, *Angew. Chem., Int. Ed.*, 2013, **52**, 9568–9571.
102 O. Santoro, F. Lazreg, Y. Minenkov, L. Cavallo and C. S. J. Cazin, *Dalton Trans.*, 2015, **44**, 18138–18144.
103 E. Blondiaux, J. Pouessel and T. Cantat, *Angew. Chem., Int. Ed.*, 2014, **53**, 12186–12190.
104 S. Das, F. D. Bobbink, G. Lanurenczy and P. J. Dyson, *Angew. Chem., Int. Ed.*, 2014, **53**, 12876–12879.
105 C. A. Dyker, V. Lavallo, B. Donnadieu and G. Bertrand, *Angew. Chem., Int. Ed.*, 2008, **47**, 3206–3209.
106 A. Fürstner, M. Alcarazo, R. Goddard and C. W. Lehmann, *Angew. Chem., Int. Ed.*, 2008, **47**, 3210–3214.
107 C. Pranckevicius, L. Fan and D. W. Stephan, *J. Am. Chem. Soc.*, 2015, **137**, 5582–5589.
108 W. Chen, J. Shen, T. Jurca, C. Peng, Y. Lin, Y. Wang, W. Shih, G. P. A. Yap and T. Ong, *Angew. Chem., Int. Ed.*, 2015, **54**, 15207–15212.
109 Z. Yang, B. Yu, H. Zhang, Y. Zhao, G. Ji, Z. Ma, X. Gao and Z. Liu, *Green Chem.*, 2015, **17**, 4189–4193.
110 G. Li, J. Chen, D. Y. Zhu, Y. Chenand and J.-B. Xia, *Adv. Synth. Catal.*, 2018, **360**, 2364–2369.
111 H.-Y. Niu, L.-J. Lu, R.-Y. Shi, C.-W. Chiang and A.-W. Lei, *Chem. Commun.*, 2017, **53**, 1148–1151.
112 X. Liu, X. Li, C. Qiao, H. Fu and L. He, *Angew. Chem., Int. Ed.*, 2017, **56**, 7425–7429.
113 R. L. Nicholls, J. A. McManus, C. M. Rayner, J. A. Morales-Serna, A. J. P. White and B. N. Nguyen, *ACS Catal.*, 2018, **8**, 3678–3687.
114 C. Chauvier and T. Cantat, *ACS Catal.*, 2017, **7**, 2107–2115.
115 S. G. Bratsch, *J. Phys. Chem. Ref. Data*, 1989, **18**, 1–21.
116 S. N. Riduan, S. Nurhanna, J.-Y. Ying and Y.-G. Zhang, *J. Catal.*, 2016, **343**, 46–51.
117 H. Lv, W.-L. Long and F.-W. Li, *Chem.–Eur. J.*, 2018, **24**, 16588–16594.
118 Q.-J. Shen, X.-H. Chen, Y.-Y. Tan, J.-Z. Chen, L.-M. Chen and S.-Z. Tan, *ACS Appl. Mater. Interfaces*, 2019, **11**, 38838–38848.
119 N. von der Assen, P. Voll, M. Peters and A. Bardow, *Chem. Soc. Rev.*, 2014, **43**, 7982–7994.
120 L. J. Müller, A. Kätelhön, S. Bringezu, S. McCoy, S. Suh, R. Edwards, V. Sick, S. Kaiser, R. Cuéllar-Franca, A. El Khamlichi, J. H. Lee, N. von der Assen and A. Bardow, *Energy Environ. Sci.*, 2020, DOI: 10.1039/d0ee01530j.